


RESEARCH ARTICLE

WILEY

Hybrid rubber-concrete isolation slab system with various shape factors for structures subjected to horizontal and vertical vibrations

Nahal Kamil Fayyadh¹ | Farzad Hejazi² 

¹Department of Civil Engineering, University Putra Malaysia, Seri Kembangan, Malaysia

²Department of Geography and Environmental Management, The University of The West England, Bristol, UK

Correspondence

Farzad Hejazi, Department of Geography and Environmental Management, The University of The West England, Bristol, UK.

Email: farzad.hejazi@uwe.ac.uk

Summary

The present framework proposed the development of a Hybrid Rubber-Concrete Isolation Slab System (HRCISS) to support building structures subjected to horizontal and vertical vibration due to ground motion and machine or equipment operation in the structure. Given that the effect of the shape factor on both horizontal and vertical stiffness has yet to be reported, the proposed composite system was comprised of two layers under the nodal points of the upper layer near the slab corners with four High Damping Rubber (HDR) components positioned between the slab layers to dissipate multidirectional (horizontal and vertical directions) vibrations. The ABAQUS software was utilized to model the finite element model (FEM) and simulate the HRCISS subjected to cyclic horizontal and vertical displacements. For the optimal HDR design, the model was applied in five 3-story buildings, and the effect of distinct shape factors ($0 < S < 2$) of the HDR bearings—the ratio of bearing's loaded area to unloaded area (free to bulge)—within the hybrid system was evaluated. For each building with a specific HDR shape factor, the HRCISS was installed in the first, second, and third stories, separately, to investigate the influence of the installation level of the isolation system on the overall structural performance. The multistory buildings were subjected to two types of vibration loads: the interior machine-induced vibrations, and the exterior seismic-induced vibrations in the horizontal and vertical directions. Based on the results, the FEM results proved the significant influence of the shape factors on the dynamic response of the HRCISS under both interior and exterior 3D vibrations when applied in multistory buildings. The lateral drift of the three-story one-bay buildings decreased with the decrement of shape factor with buildings of HRCISS installed in 1st story recording more reduction. Moreover, the deflection in the structural slab under the HRCISS decreased for lower shape factor bearings. Nevertheless, the reduced deflection was less affected by the level of the machine-equipped story. The rubber layer also stiffened in shear and compression directions with a higher shape factor.

This is an open access article under the terms of the [Creative Commons Attribution](https://creativecommons.org/licenses/by/4.0/) License, which permits use, distribution and reproduction in any medium, provided the original work is properly cited.

© 2022 The Authors. The Structural Design of Tall and Special Buildings published by John Wiley & Sons Ltd.

KEYWORDS

floating floor, high damping rubber, horizontal and vertical cyclic loading, shape factor

1 | INTRODUCTION

Elastomeric bearings are commonly utilized for vibration isolation in structural buildings. They consist, in general, of rubber layers bonded to steel shims that convey high vertical stiffness in the bearings to carry high-gravity loads. On the other hand, the total thickness of the rubber layers for a specific loaded area and shear modulus provides low stiffness in the horizontal direction that enables the bearings to shift the horizontal period, hence isolating the structure from the vibrating source.^[1] Isolation bearings are typically used for horizontal isolation purposes since it only generates flexibility in the horizontal direction, which decouples the superstructure from the substructure. However, horizontal vibrations do not exist alone but are accompanied by vibrations in the vertical direction, which should be taken into consideration since they can cause serious damage to the structural membranes that are only designed to resist horizontal action.^[2]

The horizontal and vertical vibration isolation is noted to be influenced by the loaded area and the thickness of the rubber bearings. The ratio of the loaded area to the unloaded area (side unconstrained area or area free to bulge that is dependent on the rubber layer thickness) is called the shape factor, which is a measure of local slenderness of the rubber bearing that plays a major role in the design of isolation bearings as it acquires suitable vertical stiffness. Previous studies have shown that shape factor, S in rubber bearings cause a large increment in compression modulus to a certain level, specifically for $1 < S < 24$, and the rate of increase becomes lower for $S > 24$.^[3] Given that low shape factor is accompanied by low shear and compression stiffness,^[4] low shape factor bearings with low stiffness can be utilized to provide flexibility in the vertical direction alongside the horizontal flexibility. This approach is particularly useful for low-rise buildings with low center-of-mass since they do not require higher vertical stiffness to sustain the weight. The current technique of designing multi-layered rubber bearings for horizontal seismic isolation implements thin rubber layers bonded with closely spaced steel shims, leading to shape factors ranging between 15 and 30^[5] and even as high as 37 in Japan.^[6] Although the effect of shape factor on horizontal seismic isolation has been immensely studied in the past, its impact on the vertical stiffness in fiber-reinforced isolators has only been investigated recently.^[4] Ren et al.^[7] found that distortion of more than 50% in the shape factor of rubber bearings could lead to distortions in shear stiffness, compressive stiffness, and energy dissipation, while Khaloo et al.^[8] revealed that the stiffness in high and low damping rubber bearings was less effective when the shape factor was decreased. Nevertheless, the effect of the shape factor on both horizontal and vertical stiffness has yet to be reported. It is essential to fill this research gap since the findings would present a potential solution to address the isolation of three-dimensional (3D) vibrations through effective rubber bearings.

Currently, bearings with high shape factor values are notably heavy due to their huge mass of steel layers that are vulcanized to the rubber, making it highly expensive to produce and install. In addition, superstructures isolated using bearings with high vertical stiffness result in low vibration periods, which cause deterioration in critical facilities under the effect of the vertical component of an earthquake.^[9] On the contrary, low shape factors (LSF) are aimed to achieve 3D isolation due to the low vertical and horizontal stiffness. Losanno et al.^[10] showed that both Carbon Fiber-Reinforced Elastomeric Isolators (C-FREI) and Polyester Fiber-Reinforced Elastomeric Isolators (P-FREI) with a low shape factor value of 0.625 resulted in a decent response under bidirectional seismic excitations. Moreover, Losanno et al.^[11] pointed out that low shape factors led to a limited vertical stiffness for the rubber bearings and the aspect ratio of the bearings affected the performance of the bearing under horizontal cyclic loading. Shape factor was also found to significantly influence the tension and buckling in rubber bearings subjected to the combined and fluctuating compressive or tensile loads due to the seismic excitation,^[12] whereas it was noted that the increment of the shape factor of high damping natural rubber bearings led to a slight reduction in the peak displacement of piers and decks of bridges, while the change in the shape factor value from low to high between 10 and 25 resulted in a significant alteration of the compressive and tensile forces in the bearings.^[13] It was observed by Oh and Kim^[14] that the increased shape factor increased the vertical rigidity but reduced the creep. However, creep deformation in laminated rubber bearings was found to be 0.2%–0.6% of total rubber thickness, which can be negligible.^[15] The increase in shape factor was also reported to cause augmentation in the critical displacement of laminated rubber bearings.^[16] Sunaryati et al.^[17] found that bearing with S values greater than 20 tends to be less effective in isolating motion in the horizontal direction. On the contrary, elastomeric bearings with $5 < S < 30$ provide low shear stiffness that is both suitable for horizontal isolation and high vertical stiffness for carrying huge weights. Hence, the optimum shape factor of rubber bearings is assumed to be less than 5 to sufficiently provide a relatively low vertical stiffness and compression modulus while being highly flexible in the lateral direction, although low shape factors may cause buckling in the rubber bearing, which can result in the reversal of the hysteresis curve.^[18]

Additionally, Gauron et al.^[19] revealed that the shape factor has a small influence on the buckling limits when lateral and vertical loads were subjected to rubber bearings of square sections and variable shape factors. It was observed by Oh and Kim^[14] that the increased shape factor increased the vertical rigidity. It is worth noting that typical laminated isolating bearings are installed in the base or mid-story of a building to dissipate energy that transmits from the ground motion, such as vehicle and machinery motion into the superstructure, hence providing flexibility to the structure. In contrast, isolating vibrations that transmit from upper structures into the membranes beneath is rarely seen and is conducted for

relatively low vibrating installments compared to ground vibrations. These vibration sources have low center-of-mass when compared to the overall superstructure. In turn, they do not require high vertical stiffness in the bearings to sustain such weight, which can be accomplished through the exclusion of steel shims in the isolators, thus, providing both additional flexibility to the system and a lower shape factor.^[8]

In view of the research gap and the potential use of rubber bearings with low shape factors to provide structural flexibility under horizontal and vertical vibrations, this research aimed to develop the Hybrid Rubber-Concrete Isolation Slab System (HRCISS) for structures subjected to multidirectional vibrations on various story levels. In addition, Regulation No.5 of the Malaysian Regulations for Factories and Machinery (1983) highlighted that any vibrating machinery should not be installed in floors higher than the ground level unless such floor is designed to support the load so imposed thereon. Therefore, the present research aimed to propose a HRCISS by developing a floating slab system with implementing of high damping rubber in the intermediate layer of concrete slabs. The influence of low shape factors ($0 < S < 2$) on the dynamic response of high damping rubber bearings in the HRCISS was evaluated by implementing the proposed system in a three-story one-bay building, throughout finite element (FE) simulation.

2 | DEVELOPMENT OF HYBRID RUBBER-CONCRETE ISOLATION SLAB SYSTEM (HRCISS)

2.1 | Floating slab and isolation layer design

2.1.1 | Slab and isolation layer configuration

The isolation layer was positioned between the upper (floating) slab layer and the lower (structural) slab. The dimension of the upper floating slab was $0.8 \text{ m} \times 0.8 \text{ m} \times 0.1 \text{ m}$ and reinforced with longitudinal and transverse of $\phi 10$ -mm rebars, which were designed according to ACI-318-08^[20] and EC2 (2004) guidelines. The steel reinforcement was positioned 25 mm from the bottom of each slab. Figure 1 illustrates the configuration of the floating slab layer with its reinforcing rebars.

This study proposed a square-section High Damping Rubber (HDR) bearing with a single layer of rubber designed in accordance with ISO.^[21] This was based on a previous work by Jim et al.,^[22] which demonstrated that a point-like rubber layer (such as square and rectangular section pads) was more effective in damping vertical vibrations than linear and full-surface rubber layers below the floating slab when tested under railway vibrations in the laboratory (Figure 2).

In typical isolation bearings, the rubber layers are supported with steel shims to increase the vertical stiffness and sustain massive weights of buildings. However, this study excluded the use of steel shims to obtain a low vertical stiffness that sufficiently supports low to medium machine masses. The bearing was covered with steel flanges from the top and bottom (Figure 3).

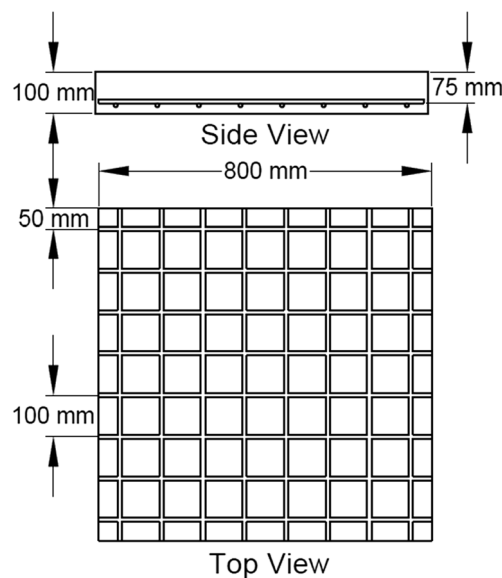


FIGURE 1 Layout of the floating slab with its reinforcement

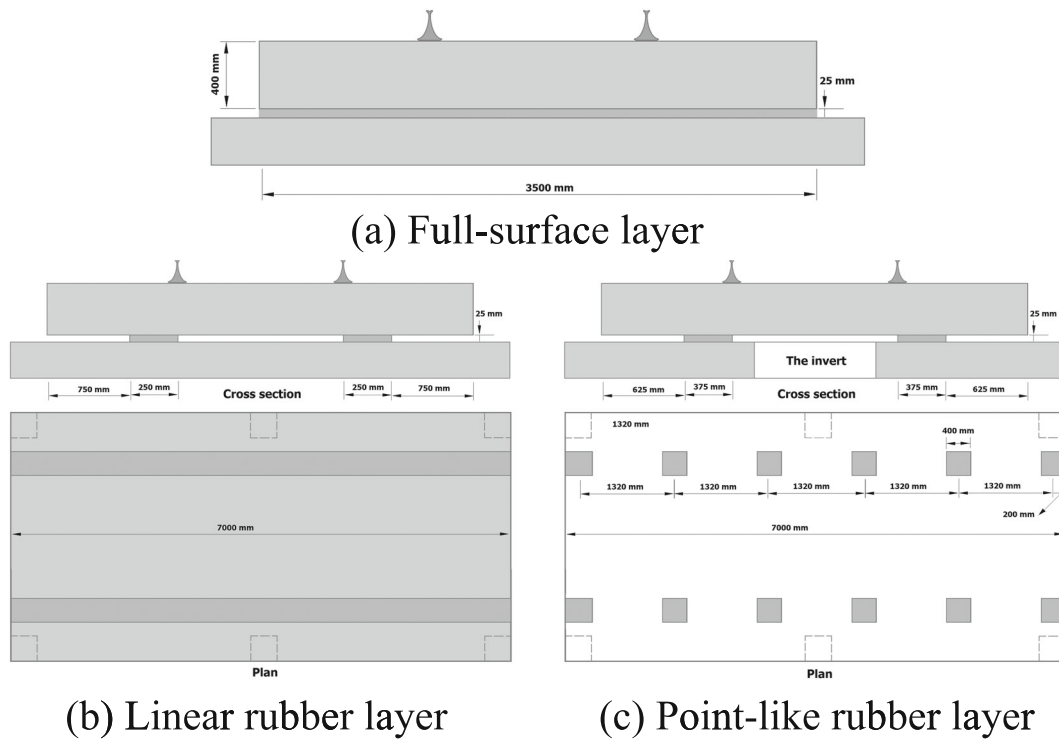


FIGURE 2 (a–c) Rubber-floating slab with different forms of rubber layer (unit: mm)^[22]

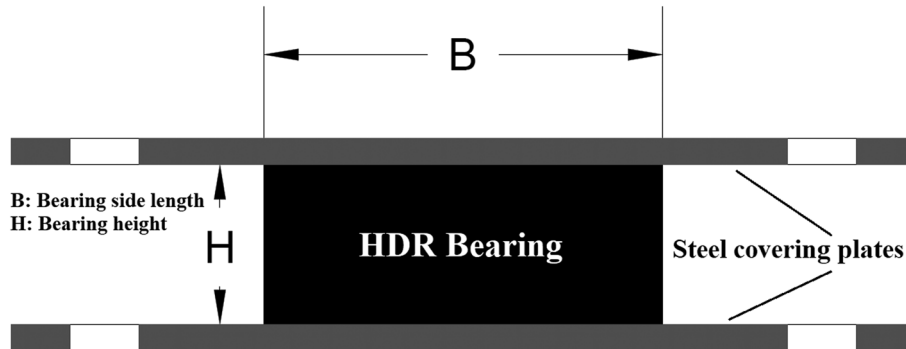


FIGURE 3 Side-view of proposed High Damping Rubber (HDR) bearing of a single rubber layer without steel shims

2.1.2 | Optimal location of rubber bearings

The proposed HRCISS in this study was developed through the combination of slab panels and HDR bearings (150 mm × 150 mm). Four HDR bearings were located below the nodal points of the floating slab (Figure 4). A nodal point is the intersection of the regions in the plate that lies between the positive and negative vibration deformation (zero deformation) of the last two shape modes.

The optimum location of HDR bearings under the floating slab was determined using a technique developed by Hui and Ng.^[23] The technique used for square plates on shaking tables at different frequencies to reduce the critical flexural vibration mode. The resulted modes of vibration were analyzed and only the modes with symmetric shapes were considered. The location of HDR bearings should be under the nodal points. This technique also proved to be applicable in the FE software by applying different frequencies on a plate and following the same steps of the experiment.^[23] These points represent the optimum HDR bearings locations to isolate vibrations on the slab.

Therefore, the ABAQUS commercial software was utilized to develop the FE model (FEM) of the considered slab panel and evaluate the slab response under applied load in various modes of vibration. The four edges of the upper slab were simply supported and the resulting shape modes were detected. The modal analysis with a natural frequency set in the steps module was performed over the floating slab layer with 10 shape modes.

Modes 8 and 9 of the response, which resulted at natural frequencies of 386.27 and 517.13 Hz, respectively, were the last two symmetrical shape modes, where their contour plot graphs (Figure 5a,b) revealed the transition regions of zero deformation (colored in blue). The combination of the blue regions of the two shape modes created four nodal points (in red circles), which were positioned at a quarter the span of the plate from each edge (Figure 5c) and highlighted the optimum location of the HDR bearings. Figure 6 demonstrates the developed HRCISS.

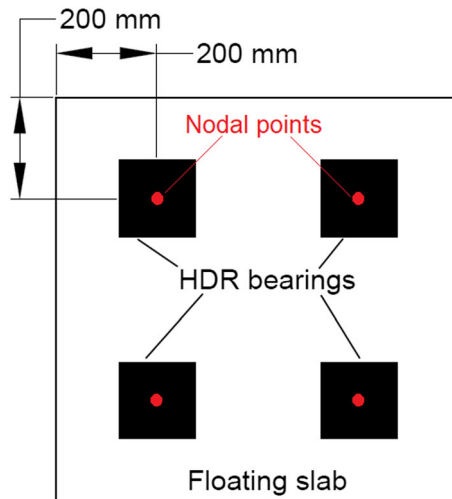


FIGURE 4 Location of High Damping Rubber (HDR) bearings at nodal points of the floating slab

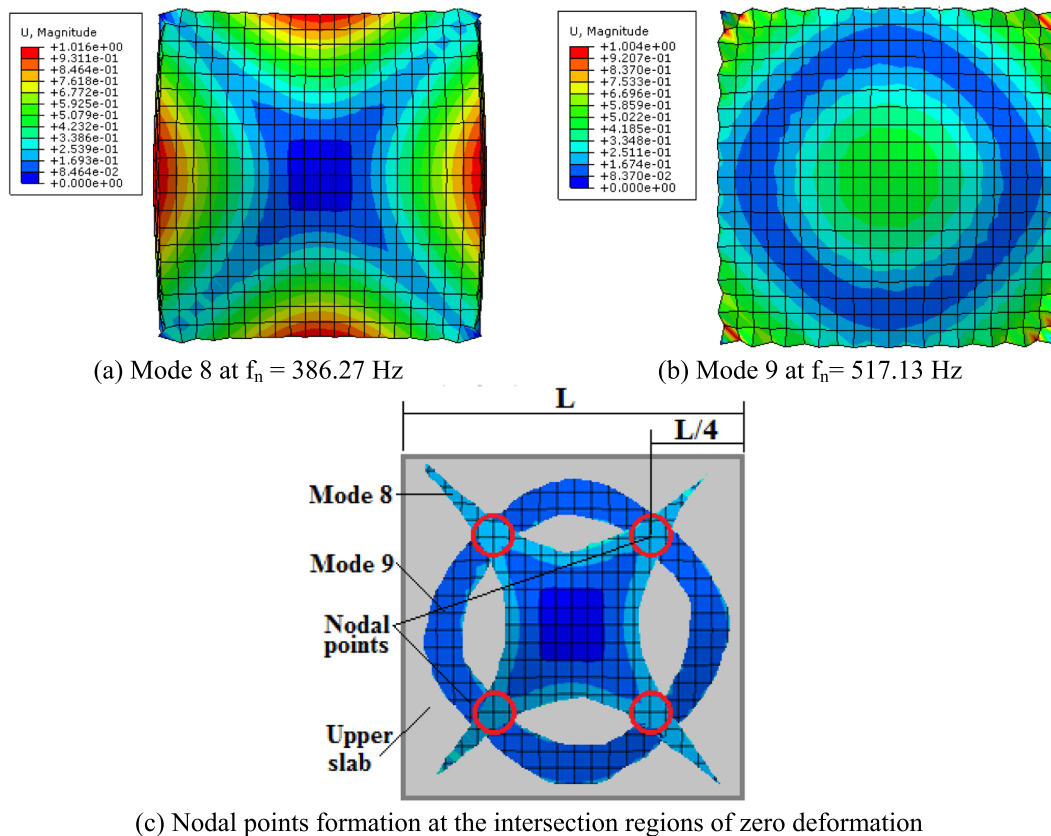


FIGURE 5 (a-c) Detecting nodal points via natural frequency test

2.1.3 | Frequency ratio and target period of the hybrid slab

By assuming the floating slab with the vibrating generator machine and isolation layer beneath as an SDOF and positioned on the structural slab as the rigid support, the dynamic force of the machine will be transmitted through the rubber layer to the rigid slab in the bottom and then to the overall frame.

The ratio between the dynamic load amplitude for the vibration generator machine to the static force (the weight of the machine) is called the transmissibility ratio (Tr), which depends on the frequency ratio, β and damping ratio, ξ . Transmissibility, as stated by Hejazi and Tan,^[24] is expressed as follows:

$$Tr = \frac{\sqrt{1 + (2\xi\beta)^2}}{\sqrt{(1 - \beta^2)^2 + (2\xi\beta)^2}} \tag{1}$$

The effect of β and ξ on the Tr is shown in Figure 7. Based on this graph, a frequency ratio higher than SQRT 2 ($\beta > \sqrt{2}$) and a damping ratio more than zero ($\xi > 0$) results in the transmissibility ratio to be less than 1 ($Tr \leq 1$). This indicates that the dynamic load due to the operation of the vibration generator machine that transfers from the slab to the frame is less than the static load of the machine.

Thus, there is no dynamic load effect of the vibration generator machine on the frame. However, a limited amount of rubber damping is required to diminish the transferred force since the use of high damping material results in high stiffness, and the system would be too rigid,

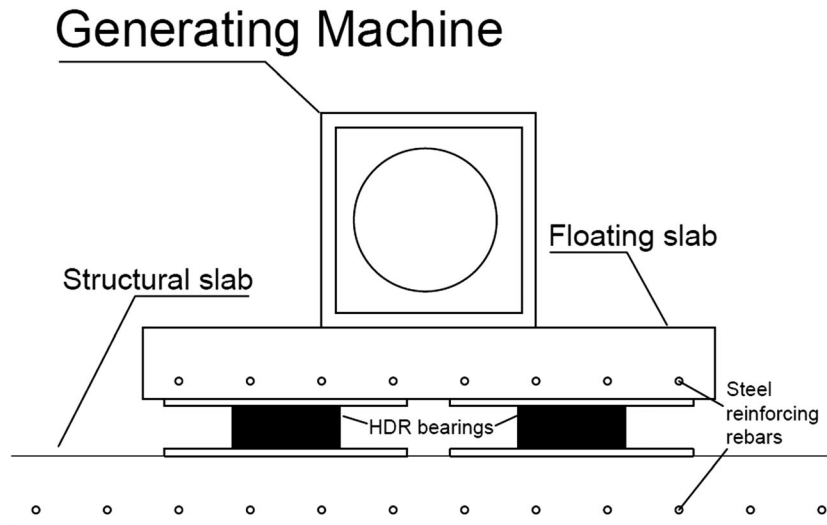


FIGURE 6 The developed Hybrid Rubber-Concrete Isolation Slab System (HRCISS) with the generating machine installed on it

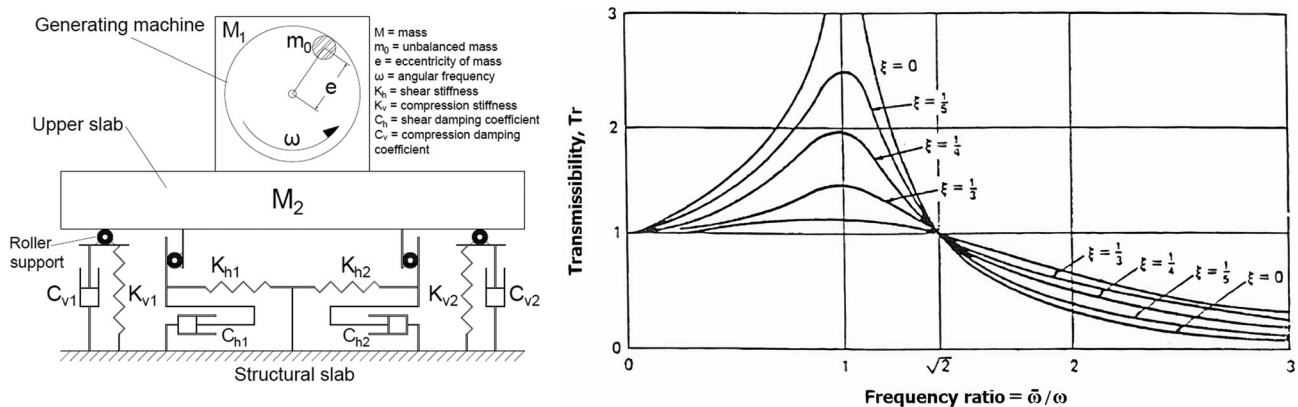


FIGURE 7 Mechanism of the proposed Hybrid Rubber-Concrete Isolation Slab System (HRCISS)

enabling all the force from the machine to pass to the bottom slab. Therefore, by considering the Tr vs. β chart, as depicted in Figure 7, the β should exceed $\sqrt{2}$ to obtain a Tr ratio of less than 1. The β is the resultant of the applied load frequency by installed equipment to the natural frequency of the system ($\beta = \omega/\omega_n$). Hence, a Tr of less than 1 can be achieved by decreasing the natural frequency of the system in comparison to the natural frequency of the vibrating machine through proper flexibility in the system. This is possible when a layer of rubber is applied between the floating slab and the structural slab beneath in which the rubber material will dampen the vibration amplitudes.

In order to examine this proposition, a natural frequency test was conducted numerically on the considered floating slab with and without a rubber isolation layer with an input machine vibration of 50 Hz (which is a typical frequency of generating machines). The results have shown the considerable decrement in natural frequency from 174.1 Hz for the frame with rigid slab system to 8.6 Hz for the frame in which the rubber layer was utilized. Then the transmissibility ratio (Tr) is determined for both slabs utilized with vibration generator machine of 50 Hz input (typical frequency of vibration generator machines). In case of rigid frame, the transmissibility ratio (which depends on frequency ratio and damping ratio), will be higher than 1 (according to the figure below), whereas the frame with rubber layer reduced the natural frequency, and since the frequency ratio (which is the forced frequency of the machine to the natural frequency of the frame) is increased; hence, Tr is shifted below 1, which indicates that output amplitudes (for structure) will be less than the input amplitudes of the machine. Figure 8 shows the two mentioned shape modes of the floating slab with and without the isolation layer. However, a β smaller than $\sqrt{2}$ results in a Tr value greater than 1, which indicates that the transferred dynamic force from the slab to the frame is more than the static weight of the machine. Since it is hazardous to the building structure, a special design is required to resist the transferred dynamic loads.

2.1.4 | Initial process for design of the HDR bearings

The HDR bearings design was based on the load and displacement capacities and the mass of the floating slab and vibrating machine. As shown in Figure 8, the natural frequency test was conducted via the FEM on the floating slab with and without the rubber layer. The presence of HDR bearings showed a reduction in the frequency, which resulted in an extended period and β that led to the decreased Tr of the system.

The dimensions of the HDR bearing design were based on the load capacity of the floating slab. The equation for the shear force capacity according to the ACI 318-08 (Section 11.11.2.1) is as follows:

$$V_c = \left(2 + \frac{4}{\beta}\right) \lambda \sqrt{f_c'} b_o d \tag{2}$$

where V_c is defined as the maximum shear force in concrete without shear reinforcement, β represents the ratio between the long and short sides of the column cross-section, f_c' is the compressive strength of the concrete, b_o is the perimeter of the support, and d is the effective depth of the slab.

Hence, the shear force capacity for a 100-mm RC slab with a 200-mm width is $V_c = 476$ kN. Since V_u is less than or equal to $0.5 \phi V_c$, where $\phi = 0.75$, the factored shear force is equal to $V_u = 143$ kN. The dimension of the HDR square bearings was calculated based on the following condition.

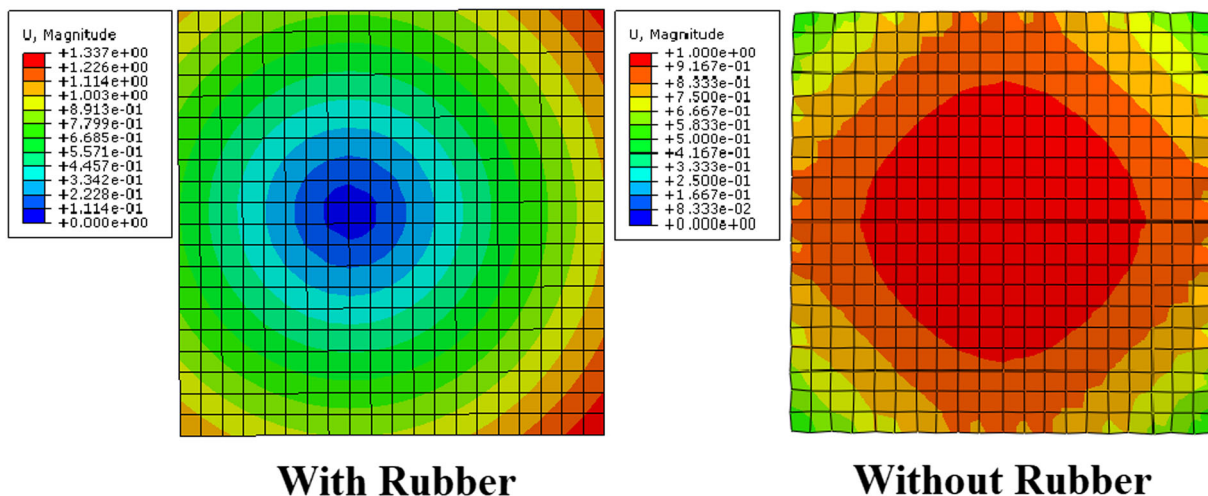


FIGURE 8 Shape modes of floating slab with and without rubber layer

The thickness of the HDR bearings was fixed to 60 mm due to the low elevation of the horizontal actuator. From Equation (2), for a 100% shear strain, the shear stiffness for a single rubber bearing was calculated as $K_h = 0.58$ kN/mm. Assuming that the shear modulus of the HDR bearing, G is equal to 0.4 and for 60-mm thickness, the loaded area of the HDR bearing, A will be approximately equal to 150 mm:

$$K_h = F/\Delta = \frac{GA}{t} \quad (3)$$

where K_h is the shear stiffness of the rubber bearing in the horizontal direction, F is the force applied horizontally on the bearing, Δ is the displacement in the horizontal direction, G is the rubber shear modulus, A is the loaded area of the rubber bearing, and t is the rubber bearing thickness.

Therefore, the HDR bearing dimensions were considered as square section with 150-mm side length, 60-mm thickness, and a shape factor of 0.625 for each bearing. The bearings were covered with steel plates with an individual section dimension of 340 mm \times 340 mm and 10-mm thickness on the top and bottom faces, which connect the bearings with the two concrete slab panels.

2.2 | Application of HRCISS

HRCISS was developed and installed within existing constructions to provide a controlled system that isolates the source of vibrations from the structural elements and eliminates the damage potential of the building. The system was designed with simple elements comprising a layer of reinforced concrete and a set of rubber bearings to disconnect the vibrating machine from the rest of the construction.

The FEM was utilized to equip the developed HRCISS in a lab-sized prototype three-story one-bay building. The multistory building was made of 3000-mm \times 3000-mm RC flat slabs of 115-mm thickness and 200-mm \times 200-mm square-section columns placed at the corners of the flat slabs. The three-story building was fixed to the ground and the HRCISS was installed to the structural slab of the building stories. The geometry and dimension of the building are shown in Figure 9. The horizontal and vertical protocols, which were in accordance with the ACI T1.1-01^[25] standard, were designed to mimic the pressing and releasing of a rotary machine. The cycles were repeated three times for the vertical protocol only. In contrast, the cycles for the horizontal protocol were not repeated during the FE simulation in order to shorten the processing time since the repeated cycles showed no outcome differences in the software.

A series of 3D interior and exterior vibrations were subjected to the building in separate test scenarios. The interior loadings consist of lateral and vertical machine-induced vibrations, as shown in Figures 10 and 11, and were applied on the midpoint of the upper (floating) slab. Since the

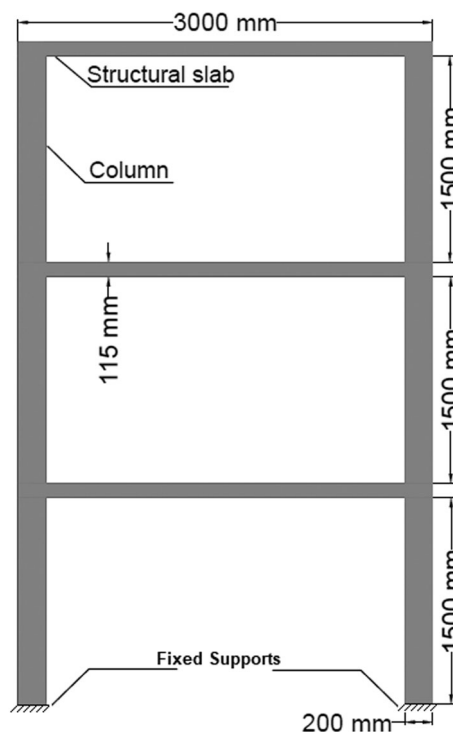


FIGURE 9 A side view of the three-story, one-bay building of RC flat slabs and square-section columns

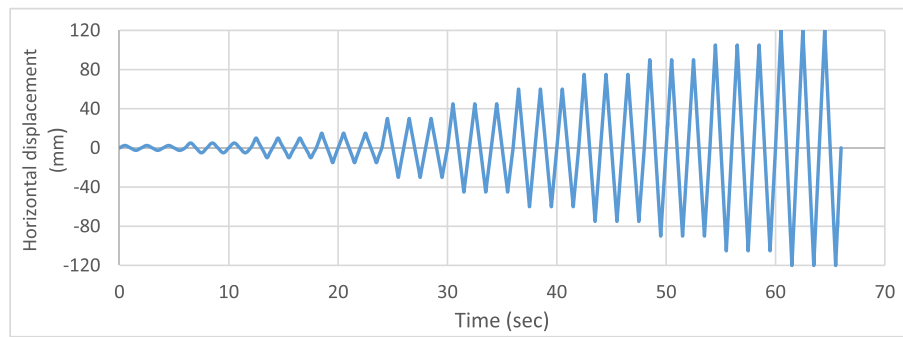


FIGURE 10 Horizontal cyclic protocol for the three-story one-bay building

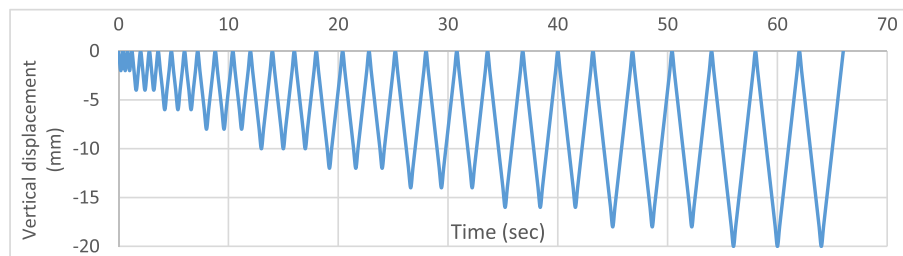


FIGURE 11 Vertical half-cyclic protocol for the three-story one-bay building

vertical stiffness of the HDR bearing was much higher than the horizontal direction, therefore, different displacement amplitudes for the machine-floating slab were defined and applied to the corresponding horizontal and vertical directions, whereas the exterior loadings that include 3D acceleration-time history components of the 1940 El Centro earthquake (Figure 12) were subjected at the base level of the buildings. Figure 13 illustrates the cyclic and seismic loadings and their application located within the three-story structure.

The lower horizontal stiffness allows the upper slab to move in a wider range during the lateral pushing and pulling, while the higher vertical stiffness restricts the vertical displacement to lower amplitude ranges. Additionally, since there was no upward movement for the slab due to the weight of the slab and the machinery, the vertical load was applied only in the downward pushing direction before the force is released to return the slab to the unloaded condition. Hence, the applied displacement history was considered as a half-cycle in the downward direction (Figure 11).

2.3 | Evaluation of the low shape factor

The effect of low shape factors ranging between 0 and 2 on the performance of the developed isolation system was investigated in a three-story building. In addition, five HDR bearings with a fixed loaded area and a thickness range between 30 and 90 mm with 15-mm increments were analyzed. Details of each of the five HDR bearings are listed in Table 1.

As mentioned in the previous section, the three-story building was subjected to interior vibrations in the form of horizontal and vertical cyclic loadings (Figures 10 and 11). The artificial vibration mimics the actual vibration of a rotary machine to assess its ability to control vibrations transfer from the machines to the structural elements, whereas the exterior vibrations in the form of seismic excitations (Figure 9) were applied at the base of the building to evaluate the capability of the HDR bearings to protect the machines from ground motion.

3 | MODELING

The ABAQUS was used as the FE software to model and simulate the proposed HRCISS and the lab-sized three-story building. The Concrete Damage Plasticity (CDP) approach was employed for the nonlinear concrete to model the slab layers using the C35/45 concrete following previous work^[26] (Figure 14).

Although the concrete performance was not expected to exceed beyond the elastic part of the nonlinear concrete since the slab was designed to resist the vibrating machine loads, the nonlinear properties of the concrete were defined during the modeling to evaluate any

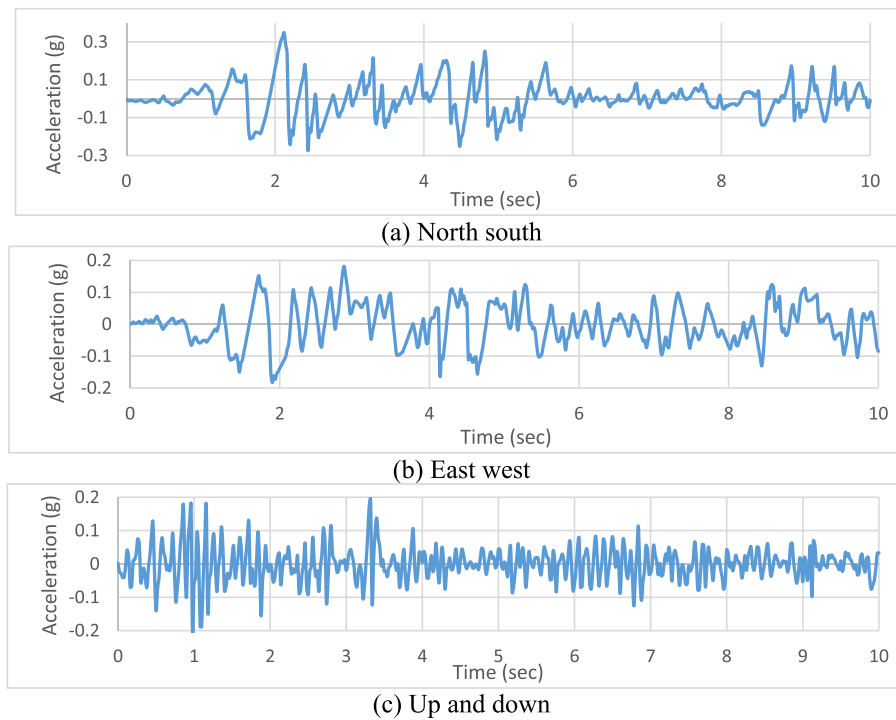


FIGURE 12 (a–c) Acceleration-time history components of El Centro 1940 earthquake

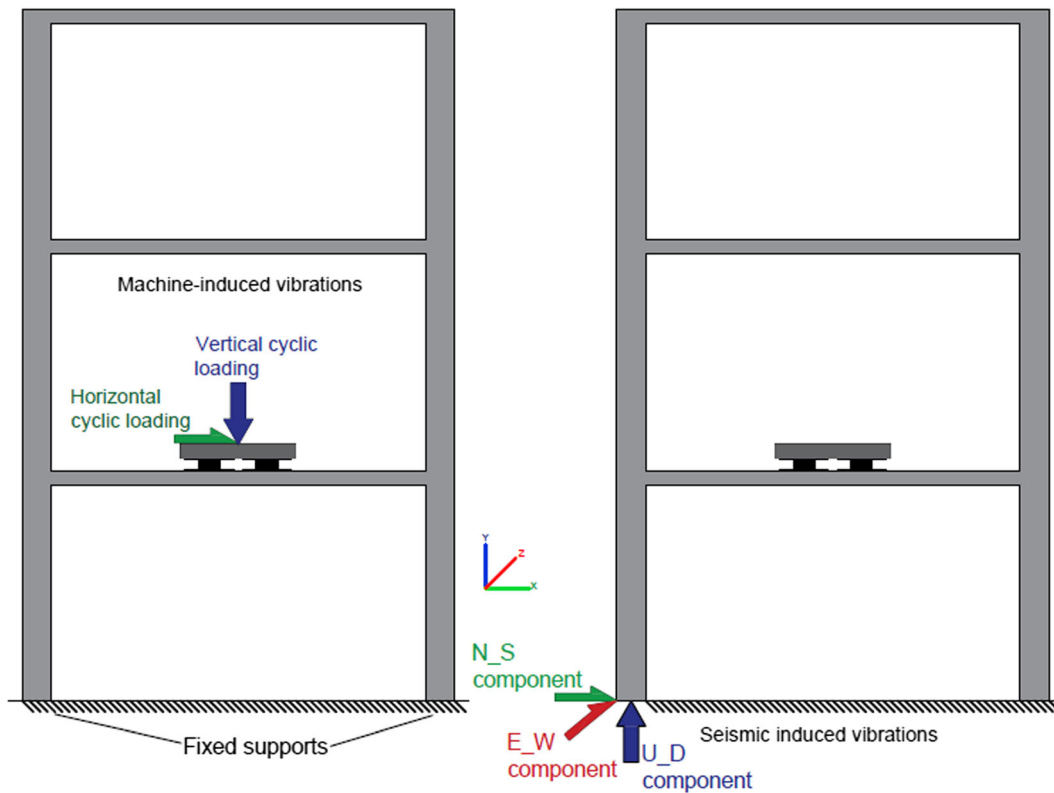


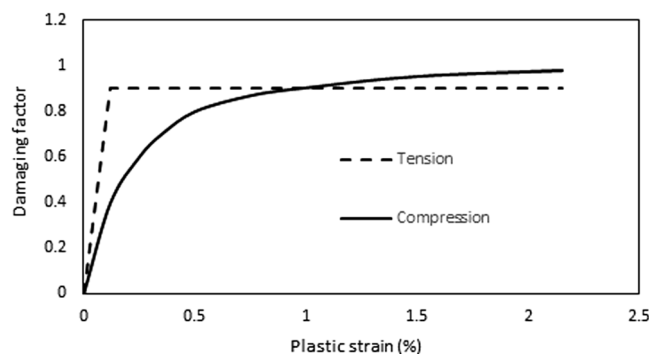
FIGURE 13 Machine-induced cyclic vibrations and seismic vibrations in the three-story building

possibility of nonlinear response under the applied cyclic loadings. The CDP model was mentioned in software documents to be designed for concrete subjected to cyclic loading. Two types of steel material were designed as reinforcement and plates with yield strength values of 400 and 600 MPa, respectively. Tables 2 and 3 list the properties of both steel and concrete used in the modeling. These values are taken from conducted

TABLE 1 Details of HDR bearings of different shape factors for 3D vibration testing

Test no.	Specimen name	Story in which HRCISS is installed	Number of HDR bearings	Side length of bearing (mm)	Thickness of bearing (mm)	Shape factor
1	3S1B-30-1	1st	4	150	30	1.250
2	3S1B-30-2	2nd				
3	3S1B-30-3	3rd				
4	3S1B-45-1	1st	4	150	45	0.833
5	3S1B-45-2	2nd				
6	3S1B-45-3	3rd				
7	3S1B-60-1	1st	4	150	60	0.625
8	3S1B-60-2	2nd				
9	3S1B-60-3	3rd				
10	3S1B-75-1	1st	4	150	75	0.500
11	3S1B-75-2	2nd				
12	3S1B-75-3	3rd				
13	3S1B-90-1	1st	4	150	90	0.417
14	3S1B-90-2	2nd				
15	3S1B-90-3	3rd				

Abbreviations: HDR, High Damping Rubber; HRCISS Hybrid Rubber-Concrete Isolation Slab System.

**FIGURE 14** Behavior of Concrete Grade C35/45**TABLE 2** Properties of steel

Steel properties	Reinforcement steel	Plates steel
Density (kg/m^3)	7850	7800
Young's modulus of elasticity, E (GPa)	210	200
Poisson's ratio, ν	0.25	0.2
Yield strength (MPa)	600	400

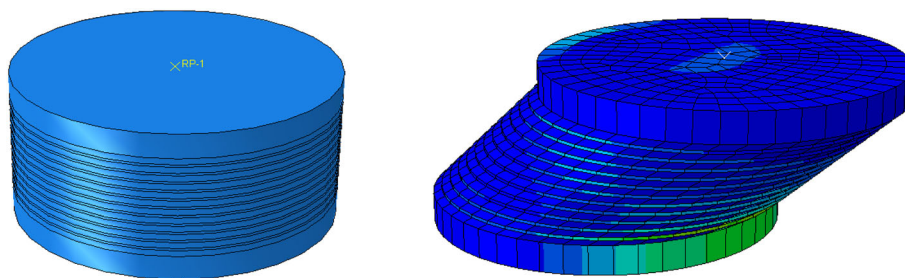
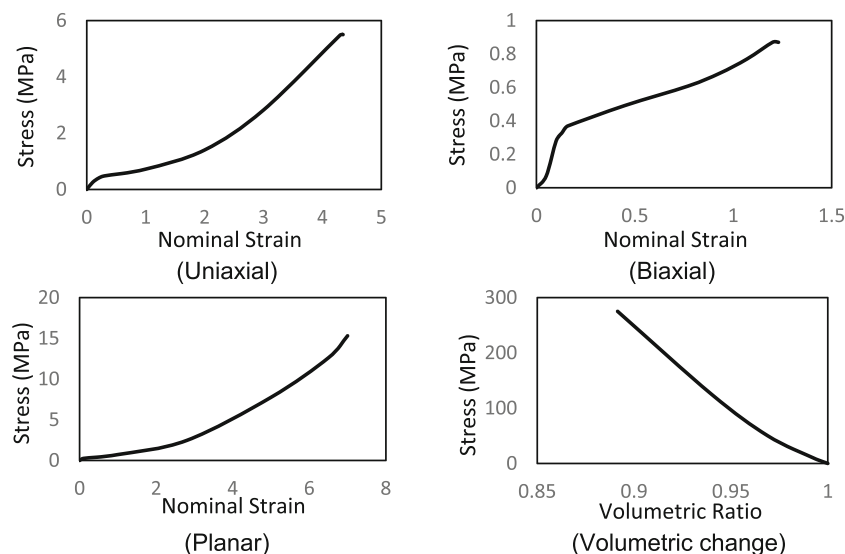
experimental tests in this study in order to validate their values in the modeling. A 3D homogeneous part with eight-node brick, reduced integration (C3D8R) element type was used to produce the concrete slab layers, bearing covering plates, and loading plate, whereas a wire type part was used to develop reinforcing rebars with T3D2 element type for meshing.

Lastly, the HDR was designed as a hyperelastic material with the coefficients obtained from the experimental test data of soft compound HDR that fits the proposed composite.^[27] The circular bearing was 125 mm in diameter and consisted of 12 layers of rubber with a total thickness of 30 mm (2.5 mm thick for each layer) and 11 layers of steel shims of 1 mm thickness with two covering steel plates with its deformed shape under horizontal shear (Figure 15).

The test data that consist of uniaxial, biaxial, planar, and volumetric change tests, as shown in Figure 16, were applied in the numerical software to determine the suitable coefficients to design the rubber material. Once the data were entered, several strain energy equations were

TABLE 3 Properties of concrete

Concrete C35/45	
Elasticity: Elastic	
Density (kg/m ³)	2500
Young's modulus of elasticity, E (GPa)	34
Poisson's ratio, ν	0.2
Plasticity: CDP	
Dilation angle	30
Eccentricity	0.1
f_{b0}/f_{c0}	1.16
K	0.6667
Viscosity parameter	0
Compressive yield stress (MPa)	45
Tensile yield stress (MPa)	3.2

**FIGURE 15** Yoo's soft High Damping Rubber (HDR) bearing re-modeled in the finite element (FE) software before and after loading**FIGURE 16** Test data of High Damping Rubber (HDR) (soft compound)^[27]

gained (Figure 17) and the coefficients of the equation with the least errors were selected. The reduced polynomial equation ($N = 2$) was used as it was stable for all cases in the FE program.

Validation for the rubber material was performed via the HDR bearing modeling and the application of the same cyclic horizontal displacement that was used in the experiment. The cyclic displacement ranged from 50% to 400% shear strain of the circular bearing. As shown in

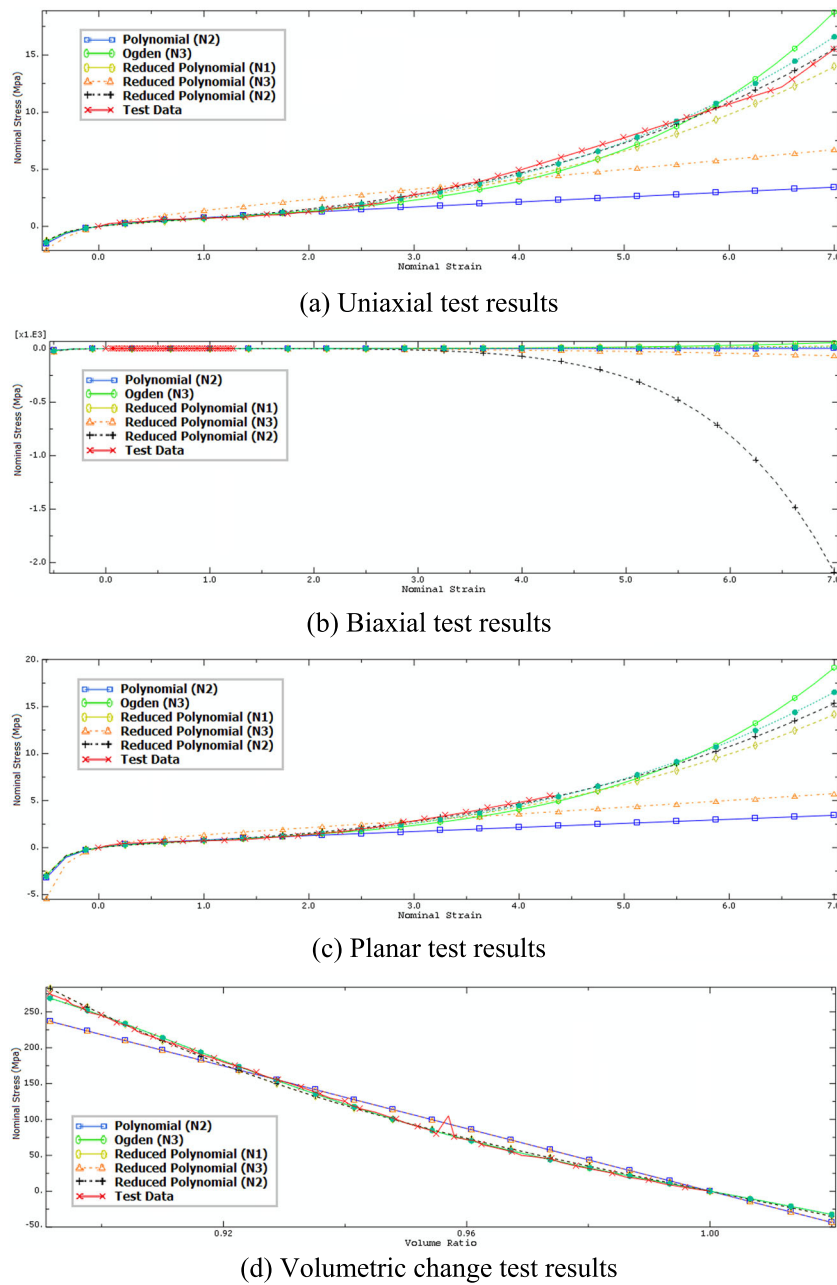


FIGURE 17 (a–d) Test results of various strain energy equations

Figure 18, the resulted reaction forces with respect to the displacement depict a strong correlation with the actual test data up to 200% shear strain (60 mm displacement), thus validating the design of the HDR model.

Figure 19 illustrates the simulated HRCISS model with the embedded steel reinforcement and the tool-meshed model, while Figure 20 shows the three-story and the HRCISS in the first story. RC flat slabs with a size of 3000 mm × 3000 mm × 115 mm were designed for the story floors, which were supported by four 200-mm × 200-mm square-sectioned columns at the corners and tied to the slabs using the Tie Constraint. Boundary conditions were set as fixed constraints at the bottom surface of the ground level columns ($U_x = U_y = U_z = 0$).

4 | VALIDATION OF NUMERICAL MODELING WITH EXPERIMENTAL TESTING

For the verification of the installed FEM in the multistory building, two identical specimens of the HRCISS were manufactured, namely, HC and VC, to validate two numerically designed HRCISS specimens, HF and VF; for cyclic horizontal and vertical testing, respectively. The dimensions

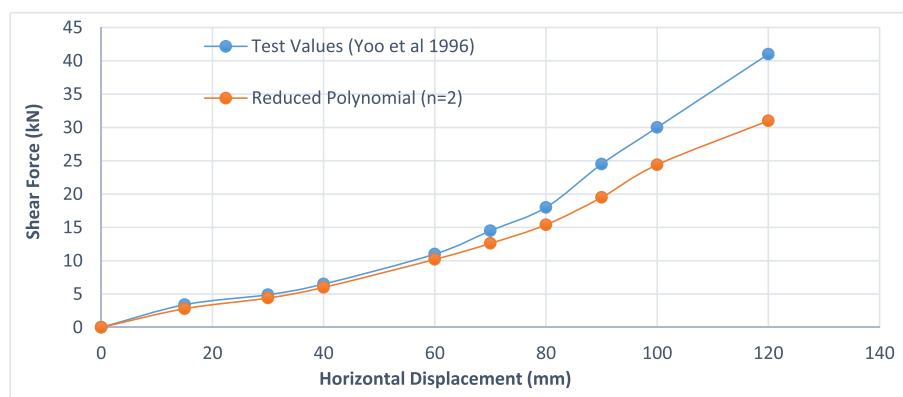


FIGURE 18 Shear force-displacement values for test results and the finite element (FE) results

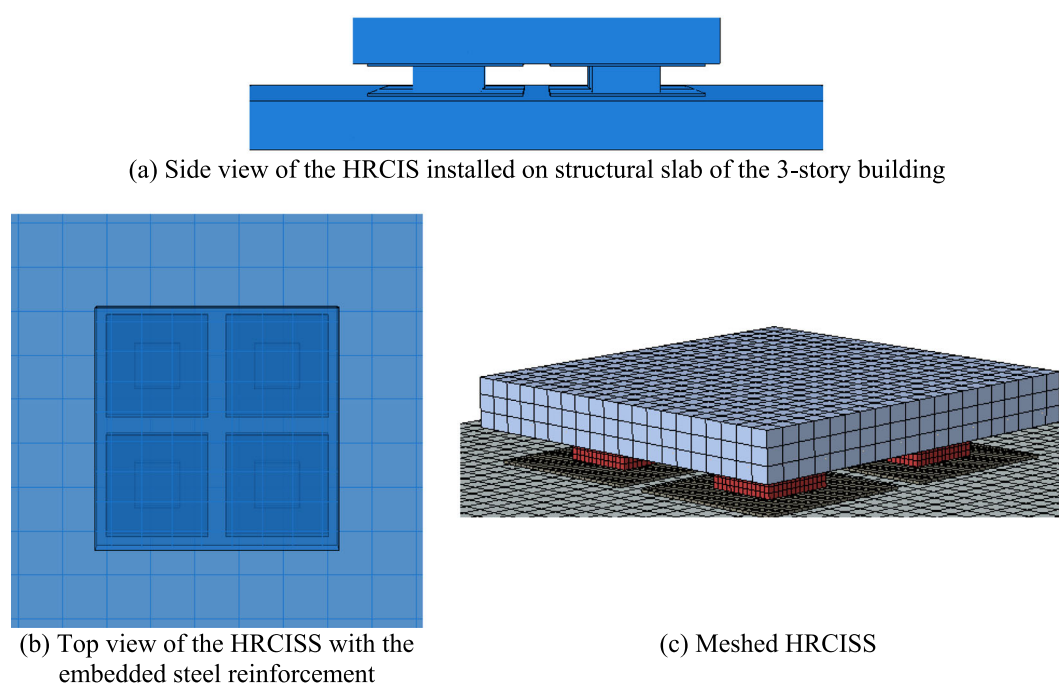


FIGURE 19 (a–c) The numerically simulated Hybrid Rubber-Concrete Isolation Slab System (HRCISS) specimen

were similar to the 3S1B-60 building from Table 1. First, the two FE specimens, HF and VF, were tested numerically under cyclic displacement-controlled loads. Then, the two specimens were manufactured using the materials, as shown in Table 4.

The four HDR bearings were connected to the slab layers by $\varnothing 20$ -mm steel bolts that have already been embedded in the concrete during the specimen casting. Steel shims were absent in the HDR bearing for the two specimens to reduce the compressive stiffness of the bearings (Figure 21).

In each slab layer, the longitudinal and transverse bars were in the same length and number and welded together to form a mesh. The reinforcement of the upper slab (for the horizontal testing) was placed 25 mm from the top face of the mold during the casting of the concrete since it will be flipped upside down once it is connected to the HDR bearings. This ensures that it is positioned 25 mm from the bottom face of each slab layer during the two testing procedures. Figure 22 shows the reinforcement in the wooden mold before casting in each slab layer was performed. A 300-mm square steel plate with 10-mm thickness was placed in the top face of the upper concrete slab layer during the casting process. It was then connected to the steel mesh layer via U-shaped steel bars and welded to both the steel plate and the mesh, as the upper layer was flipped upside down and tied above the lower layer (Figure 23). The plate was connected to a steel I-beam, which in turn was tied to the horizontal actuator before the test was performed. In addition, $\varnothing 20$ -mm steel bolts were bent into an L-shape and welded to the steel mesh pointing upwards in each slab for the lateral displacement test and extended 20 mm out of the slab surface to pass through the holes and tied in the steel

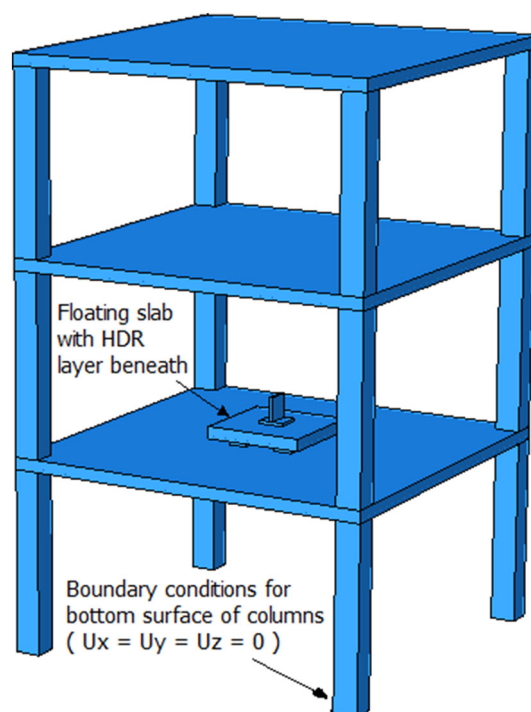


FIGURE 20 3D model of the three-story, one-bay building with Hybrid Rubber-Concrete Isolation Slab System (HRCISS) in the first story

TABLE 4 Physical material properties

Type	Shear modulus (MPa)	Compressive strength (MPa)	Tensile strength (MPa)	Young's modulus (GPa)	Elongation at break (%)	Tear resistance (kN/m)
Soft HDR	0.4–0.6	-	≥13	-	≥400	≥7
Concrete	-	46.94 (28 days)	3.2	34	-	-
Steel	-	-	677	210	-	-

Abbreviation: HDR, High Damping Rubber.

covering plates of the HDR bearings. In addition, four plastic tubes with 50-mm diameter and 150-mm thickness were placed at the corners of the mold with 100-mm distance apart from each other to create 50-mm holes to fix the lower slab to the strong floor via \varnothing 50-mm bolts during the test. However, for the vertical displacement test, the bolts were omitted since the HDR bearings undergo vertical motion, which prevents any slab lateral movement over the bearings (Figure 24).

Experimental testing using the horizontal and vertical dynamic actuators was conducted on the HC and VC specimens. Two dynamic actuators comprising the MTS and Shimadzu dynamic actuators with 300 load capacity (Figure 25) were employed to examine the dynamic response of the proposed HRCISS specimens in the vertical and horizontal directions, respectively. A loading plate was placed on the top surface of the upper slab to transfer and distribute the vertical actuator force to the upper slab. The lower slab of specimen HC was fixed to the strong concrete floor via 50-mm steel bolts that extended 100 mm above the lower layer of the top face. Thus, the dimension of the upper layer was minimized to avoid contact with the bolts during the lateral pushover and pullover phases. The horizontal actuator was linked to the top face of the upper layer using a steel link with an I-section beam and two plates; one was bolted to the actuator and the other was bolted to the perpendicular plate connected to the top of the slab panel. Meanwhile, the specimen VC was supported at the four corners of the steel supports with a size of 200-mm \times 200-mm plan and loading was applied on a steel plate that was in contact with the top face of the upper slab layer. The horizontal cyclic protocol was designed with a maximum amplitude of 60 mm due to the limited range of the horizontal actuator. The vertical half-cyclic protocol was similar to that in Figure 11. Specimen HC was tied to the strong floor and connected to the horizontal actuator via a steel I-beam welded to the upper slab loading plate (Figure 26a), while specimen VC was simply supported and the actuator was in contact with the loading plate tied to the upper slab (Figure 26b).

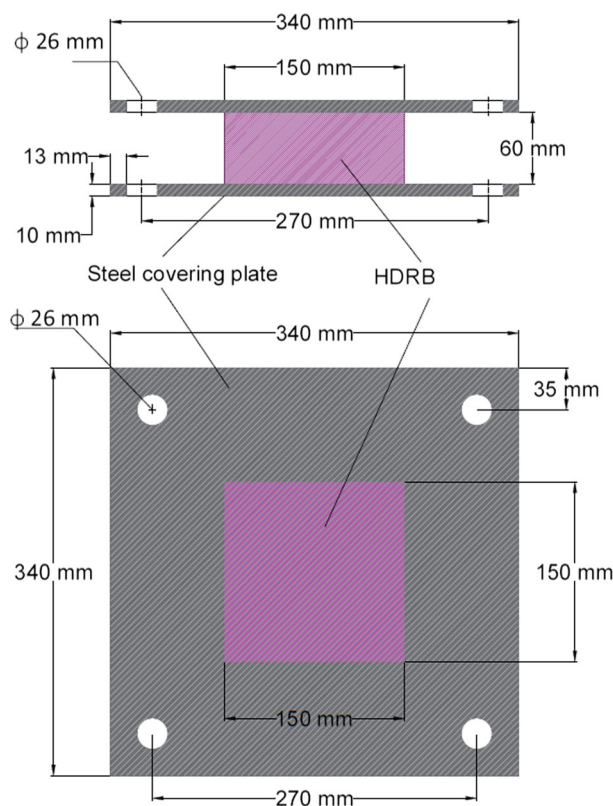


FIGURE 21 Side view and top view of rubber bearing for half-cyclic compression test

The comparison between the numerical and experimental results in terms of the force-displacement and deflection of the lower slab showed good agreement for both horizontal and vertical cyclic testing, respectively. However, the shear force reaction of specimen HC showed a decline in the last cycle, which could be due to the shear punching failure in the concrete. Figures 27 and 28 present the similarities in the force-displacement backbones for HC and HF and VC and VF as well as the deflection of the structural slab for VC and VF. Although the backbones diverged at some displacements, the errors in values were less than 10%. Thus, the model can be utilized to investigate the effect of shape factors within the multistory building.

5 | FEM RESULTS OF THE SHAPE FACTOR EFFECT

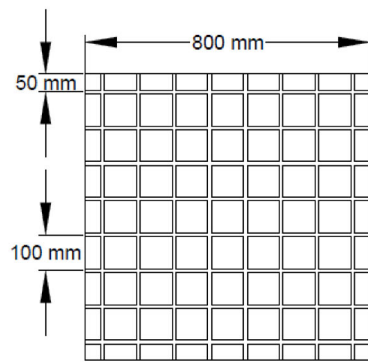
5.1 | Interior vibrations testing

Interior vibrations include the vibrations induced by the generating machines and acting on the foundation slab beneath them. These vibrations are transferred into the structural slab and may cause damage to the whole building. Therefore, the HDR bearings in the hybrid system were installed to isolate the machine and its foundation slab (the floating slab) from the structural elements of the multistory building in order to dampen the vibration amplitudes. By maintaining the same loaded area of the HDR bearings, the effect of the bearing thickness on the isolation was examined for five shape factor values.

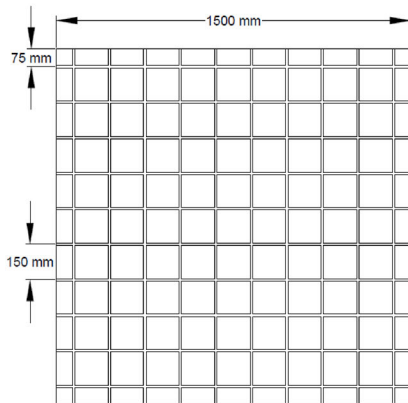
5.1.1 | Shape factor effect under horizontal cyclic loading

The FE testing on the three-story one-bay building was performed by subjecting the floating slab of the HRCISS to the horizontal cyclic displacement-controlled loading on a reference point (RP). The RP is the midpoint of the steel loading plate that is attached to the top face of the upper slab. The shear force was measured as the reaction force to the applied horizontal cyclic displacement on the upper slab.

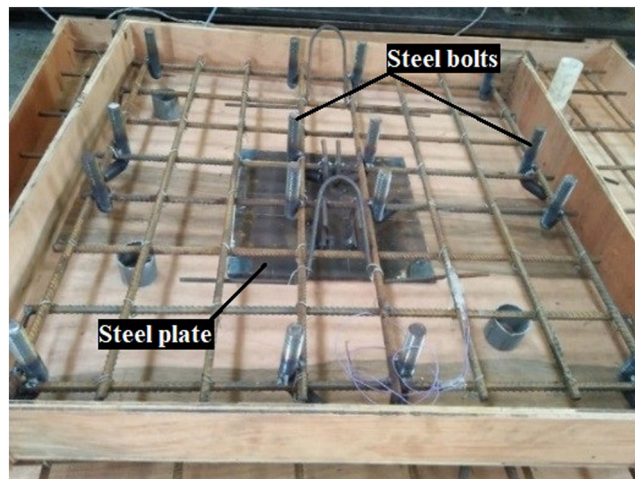
The results revealed the influence of the varying shape factor on the dynamic response of the HRCISS. A closer look at Figure 29 shows that the shear reaction force is high during the pushover and low during the pullover. This difference creates hysteretic loops, which indicate a certain



(a) Upper slab reinforcement



(b) Lower slab reinforcement

FIGURE 22 (a and b) Details of steel mesh**FIGURE 23** Steel bolts and steel load plate embedded inside upper slab for horizontal test before casting

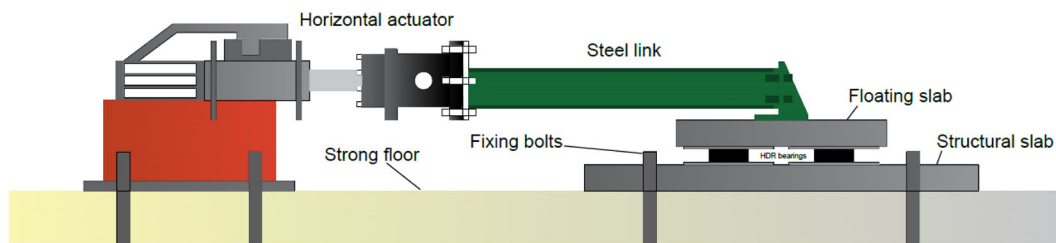
degree of damping in the rubber. The distinct force-displacement hysteretic loops of each specimen highlight roles of shape factor and story level in which the machine is installed on the shear stiffness, particularly the damping and deformation, which are discussed in the following section.

a. Shear stiffness

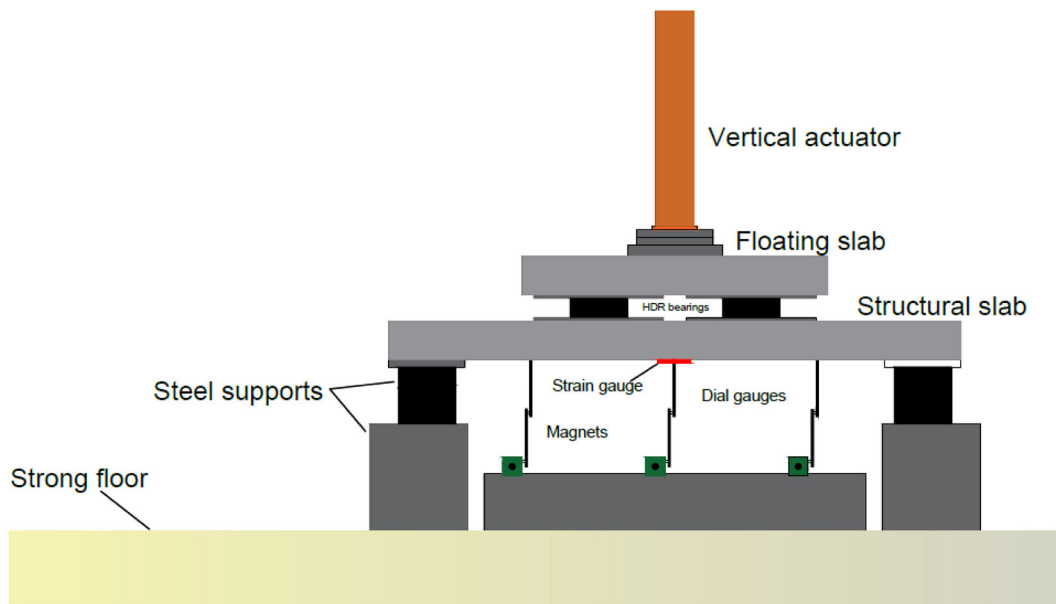
Shear stiffness is defined as the peak shear force divided by the respective maximum horizontal displacement. For buildings with HRCISS in the same level, the effect of the shape factor was exceptional, where HDR bearings provided less shear stiffness when their shape factor was



FIGURE 24 Lower slab after casting



(a) Specimen HC under horizontal actuator



(b) Specimen VC under vertical actuator

FIGURE 25 (a and b) Schematic test setup layout

decreased. This was valid for all buildings with the same level of the hybrid system. The reduced shape factor indicates the thicker HDR bearing, which increases the shear strain for a certain amount of stress and may result in lower shear stiffness in the bearings. Figure 30 illustrates the shape factor effect of different HRCISS level. Although the shear stiffness of the rubber bearings in the second and third stories increased slightly

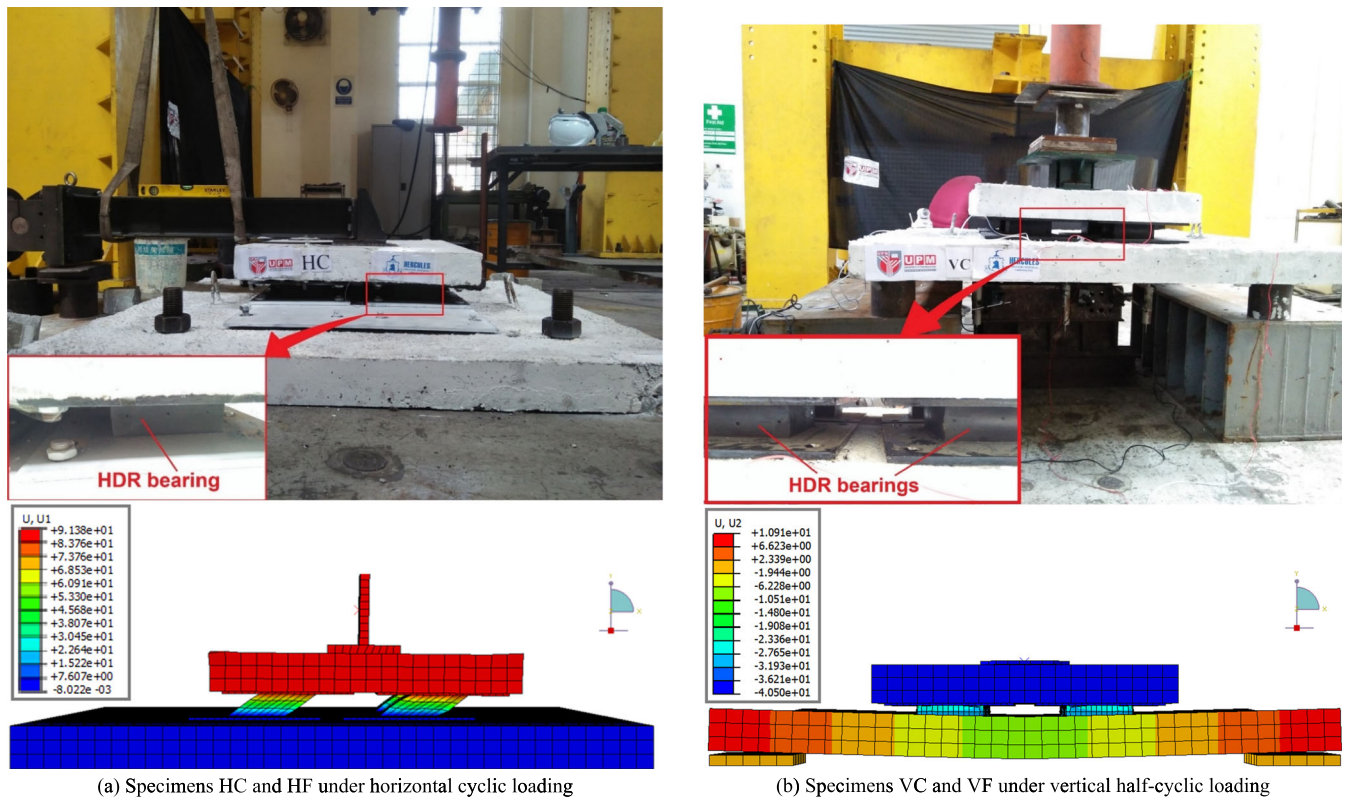


FIGURE 26 (a and b) Comparison between experimental and finite element (FE) specimens testing

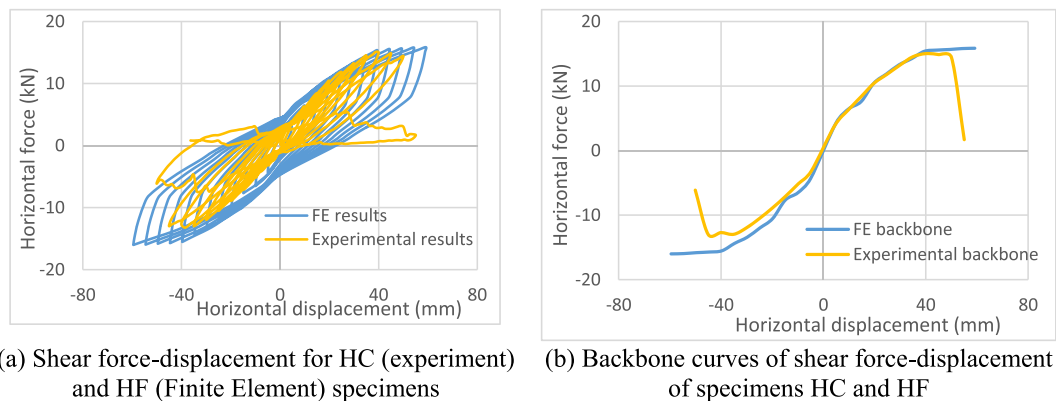


FIGURE 27 (a and b) Comparison in response between HC and HF

with the increase of the shape factor, the HDR layer in the first story showed a drastic augmentation in shear stiffness from 0.323 to 0.677 kN/mm as the shape factor increased.

Moreover, a higher story level of HRCISS led to a lower shear stiffness of the HDR bearings up to a certain shape factor. This could be due to the different masses carried by the structural slabs of the respective level. In general, lower stories carry greater masses compared to upper stories, which can intensify the reaction forces on the floating slab and subsequently lead to higher shear stiffness.

b. Shear energy dissipation and damping ratio

The hysteresis in the shear force-displacement indicates a certain amount of energy being dissipated and in turn a certain degree of damping. It was observed that HDR bearings with higher shape factors dissipated more energy and the vibration was more damped. However, the energy dissipated was much higher in the second story bearings with shape factors up to 0.625, followed by the first and third story bearings, respectively. In contrast, the energy dissipated was greater in lower stories when the shape factor values were above 0.625 (Figure 31a). This is due to

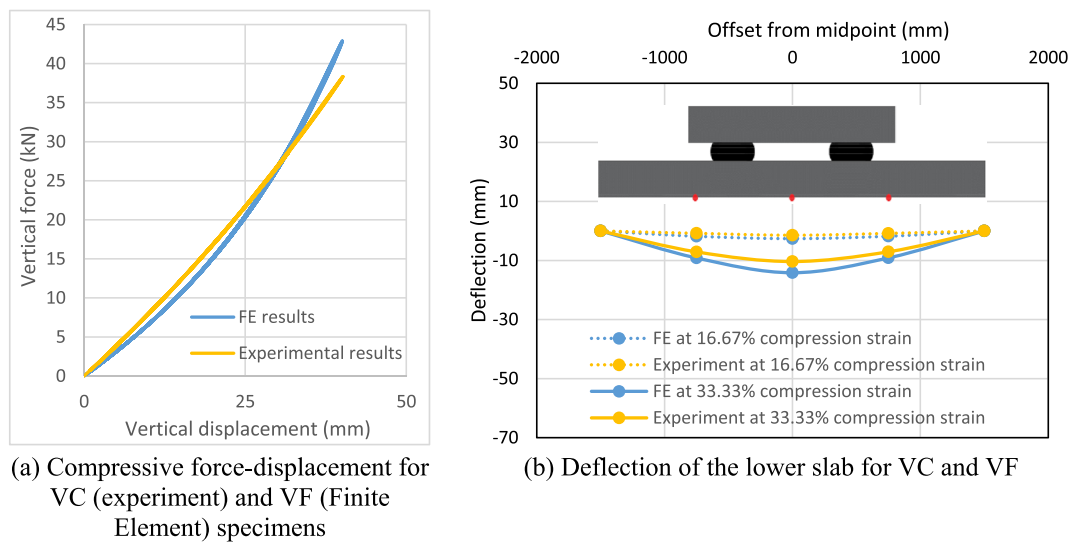


FIGURE 28 (a and b) Comparison in response between VC and VF

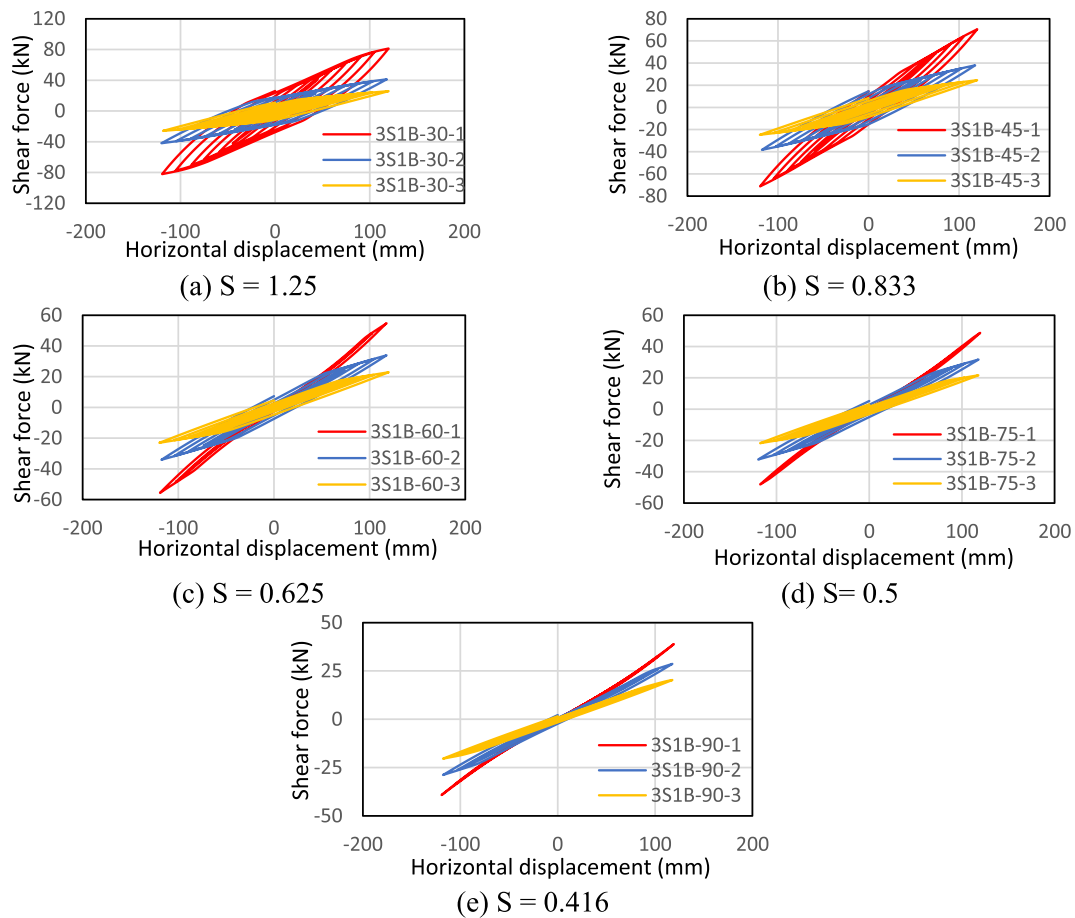


FIGURE 29 (a–e) Shear force-displacement for buildings with HDRBs of different shape factor and different story level installation

variation of the base shear distribution on the different story levels. When the bearings are mounted in the second or third story levels (where shear is lower), the bearings with lower shape factors (less shear stiffness) are able to perform better in dissipating the low shear energy in those levels. However, in the opposite case, when the bearings are installed in the 1st story level (where the shear is at its highest value), the bearings

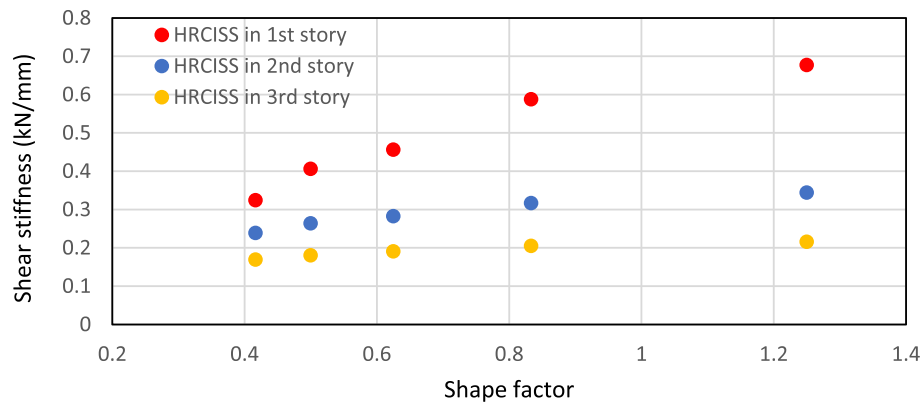


FIGURE 30 Effect of bearings shape factor on shear stiffness of Hybrid Rubber-Concrete Isolation Slab System (HRCISS) in different story levels

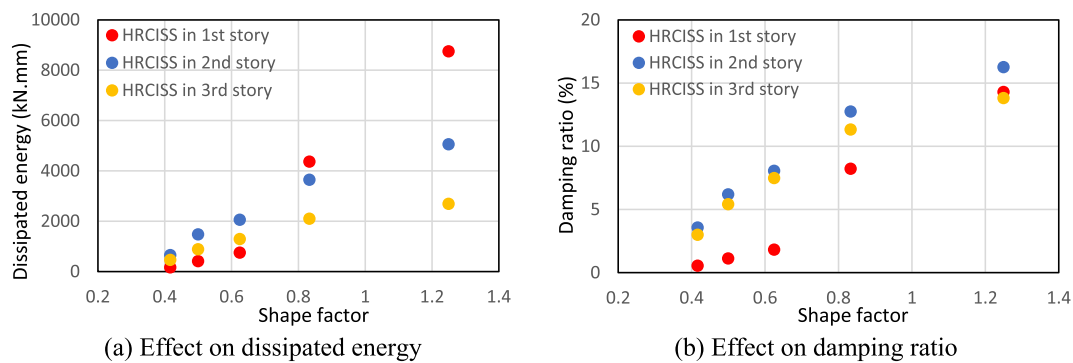


FIGURE 31 (a and b) Dissipated energy and damping ratio for Hybrid Rubber-Concrete Isolation Slab System (HRCISS) bearings with different shape factors and installed in different story levels

with higher shape factors (higher shear stiffness) dissipate the shear energy in that level more efficiently. Similarly, the respective damping ratio in the hybrid system was largely affected by the shape factor, as demonstrated clearly in Figure 31b. A higher shape factor caused more vibration to dampen at certain HRCISS level. It was also found that the damping was higher for the mid-story hybrid system compared to the upper and lower stories. This finding was associated with the fixed middle structural floor from top and bottom faces, which led to a more stable hysteretic performance of the HDR bearings.

c. Shear deformation

The applied horizontal cyclic loading on the floating slab of the three-story one-bay building with different shape factors and machine story level resulted in the lateral story drift in the positive and negative directions (Figure 32). The shape factor largely affected the story drift of the building, while the different installation levels of the HRCISS led to a distinct story drift pattern, as depicted in Figure 33. When the HRCISS is installed in the higher levels (third level), the lateral drift of the rooftop decreases in comparison to the structure drift when the HRCISS is installed either in first or second levels. Although the rooftop drift was the least for building with rubbers mounted in the third story, the lateral inter-story drift in the lower stories of the building is less than the inter-story drift of the top story, which results in rotation in columns of the top story to be more than rotation in columns of the lower stories. HDR bearings with lower shape factors caused the least lateral drift in the building stories, signifying the impact of the shape factor on the drift for HRCISS in lower stories. In short, the lower the levels of the hybrid system, the less the columns rotate. The Lateral Story Displacements (LSDs) of the multistory building with the hybrid system of different shape factors showed the impact of the HDR on reducing the deformations compared to the lateral drifts in conventional buildings. Table 5 lists the maximum LSDs of each building story and the reduction value with respect to the conventional building. Apparently, the HDR was more effective in reducing the lateral drifts, especially for higher shape factors, when the hybrid system was installed in lower stories. The result could be due to the shorter distance between the ground level and the source of vibration, which creates less momentum on the building and hence less rotation and drift.

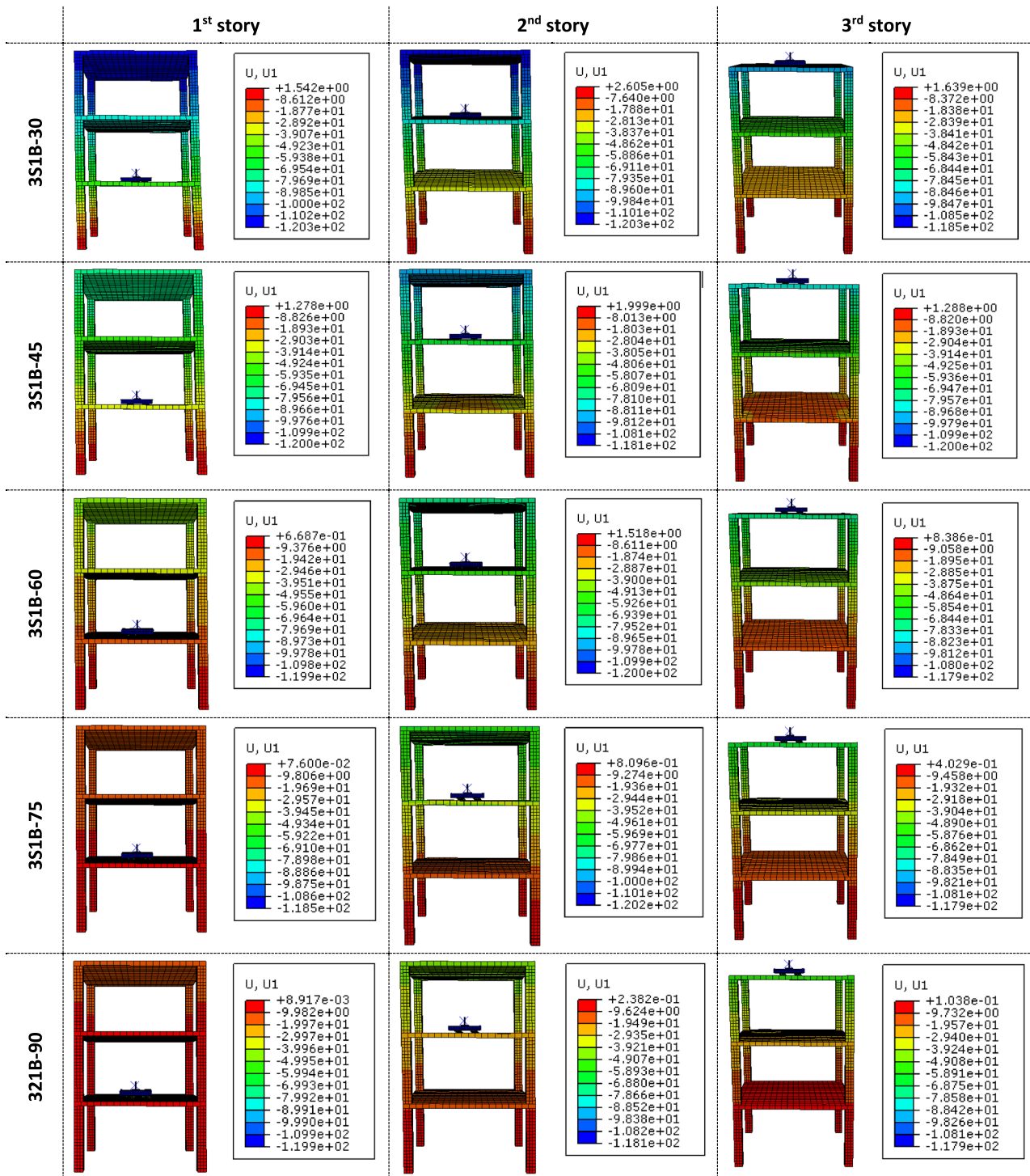


FIGURE 32 (a–e) Lateral deformation of three-story one-bay buildings with different bearing shape factors and machine-equipped story level

When the HRCISS is installed in the higher levels (third level) the lateral drift of the rooftop decreases in comparison to the rooftop drift when the HRCISS is either installed in first or second levels. Although the rooftop drift was the least for building with rubbers mounted in the third story, the lateral inter-story drift in the lower stories of that building is less than the inter-story drift of the top story, which results in columns of the top story rotating more than the lower stories columns, whereas for the building with rubber bearings installed in the first story, the rooftop drifts the most but the lateral inter-story drift of the lower stories is bigger, and hence, the columns will rotate less in the top story.

Based on Figure 34, higher shape factors caused more increment in the lateral story drift when the hybrid system was installed in lower stories. The drift increment remained low as long as the hybrid system was installed at upper stories. In addition, the differences in drift values of the three stories were less compared to multistory buildings with lower-level systems, signifying fewer inter-story drifts and as a result, less

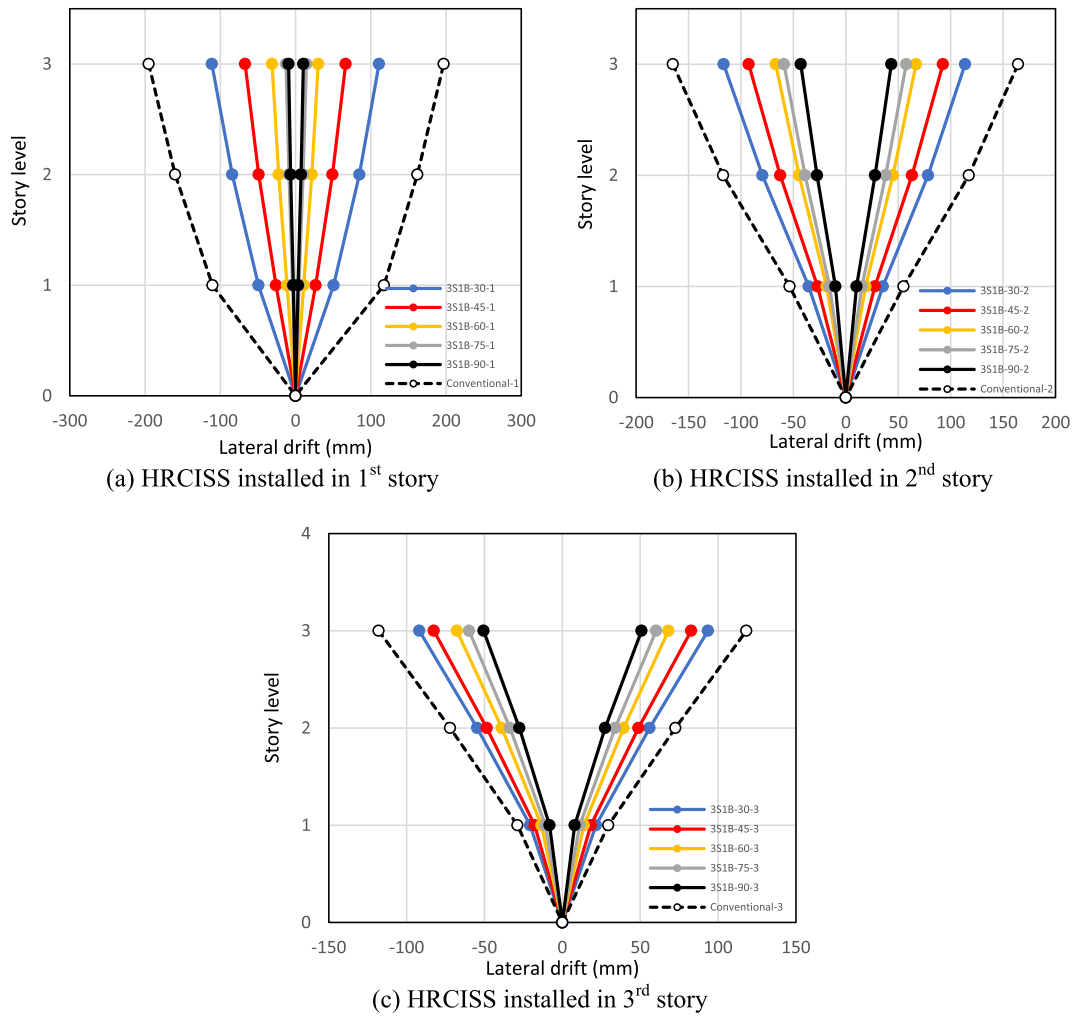


FIGURE 33 (a–c) Maximum lateral drift of each story of multistory buildings with different bearings shape factors

TABLE 5 Reduction values percent of LSD of hybrid buildings with different shape factors compared to LSD of conventional building

HRCISS-equipped story	Story	Reduction in lateral drift with respect to conventional building (%)				
		$H = 30\text{ mm}$ $S = 1.25$	$H = 45\text{ mm}$ $S = 0.833$	$H = 60\text{ mm}$ $S = 0.625$	$H = 75\text{ mm}$ $S = 0.5$	$H = 90\text{ mm}$ $S = 0.416$
1st	1st	56.98	77.28	90.69	96.04	97.16
	2nd	47.64	69.69	86.64	93.78	95.51
	3rd	43.61	66.14	84.69	92.69	94.71
2nd	1st	35.74	49.59	65.75	72.21	81.32
	2nd	33.14	46.24	61.68	67.6	76.2
	3rd	30.71	43.63	59.19	64.92	73.55
3rd	1st	26.69	38.03	53.09	62.12	73.17
	2nd	22.8	32.68	45.81	53.31	62.13
	3rd	20.88	30.02	42.32	49.02	56.95

Abbreviations: HRCISS Hybrid Rubber-Concrete Isolation Slab System; LSD, Lateral Story Displacement.

column rotation. This finding was the opposite for higher story-level isolation systems, where the upper story drifts further from the lower story and resulted in higher column rotations and more vulnerability to structural damage.

5.1.2 | Shape factor effect under vertical half-cyclic loading

The application of the vertical half-cyclic loading on the floating slab in the multistory building has a relatively similar effect on the deflection of the structural slab, regardless of the hybrid system level. The same outcome for the buildings with machine equipped in the first, second, and third stories elucidates that the level of the story is not very influential on the performance of the hybrid system under compressive cyclic loading.

a. Compressive stiffness

The compressive force resistance (stiffness) of each hybrid system is presented in Figure 35. These force-displacement relationships represent the behavior of the HDR bearings with different shape factors under the half-cyclic loading on the floating slab. A slight drop in the reaction force was detected for all specimens during the force releasing stage, which clarifies the absence of the hysteretic loops and the approximately linear action. Similar to the shear stiffness, the compressive stiffness was directly proportional to the shape factor, as observed in Figure 36. This

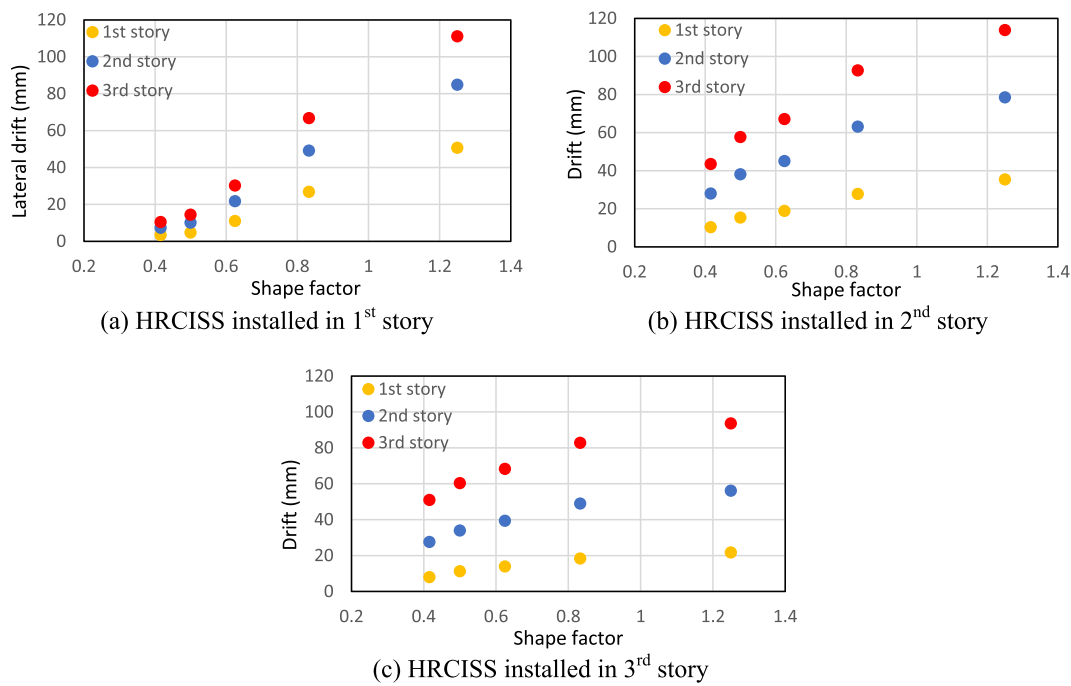


FIGURE 34 (a–c) Effect of bearings shape factor on maximum Lateral Story Displacement (LSD) in multistory buildings in different story levels

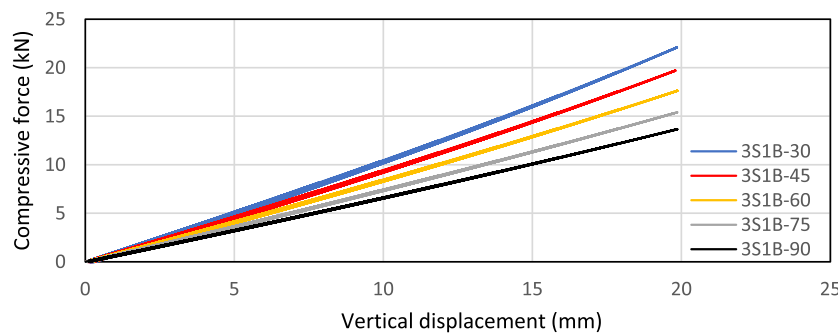


FIGURE 35 Compressive force-displacement in multistory building with different shape factors under vertical half-cyclic loading

reveals that the system is more flexible with a lower shape factor due to the thicker rubber at the loaded area, which can minimize the transfer of vibration to the structural slab and eventually reduce the deflection.

b. Compressive energy dissipation and damping ratio

Comparable to the compressive stiffness, the energy dissipation in the HDR bearings increased with the increasing shape factor (decreasing rubber thickness), which in turn led to more damping. This was probably due to the increased vertical stiffness that produced higher compressive force for a certain compressive strain and hence augmenting the dissipated energy. Figure 37 displays the dissipated energy and damping values with respect to the shape factor values. The findings showed that energy was stored when the rubber was thicker rather than being dissipated. Nevertheless, the amount of dissipated energy was very low and negligible.

c. Compressive deformation

Although thicker rubber led to less damping and reaction force on the floating slab, the resulting deflection decreased in the structural slab beneath. Figure 38 highlights the vertical deformation in the midpoint of the floating and structural slabs for each shape factor value.

The two deformation lines in the figure represent the vertical displacement of the floating slab and the deflection of the structural slab, respectively. Despite that the deformation in the 3S1B-30 specimen was reduced by only 0.9%, the reduction in deformation rapidly increased by 34.73% for the 3S1B-90 specimen.

Furthermore, the deflection in the edges, quarter-points, and midpoints of the structural slabs of different shape factor systems are depicted in Figure 39. The results showed that HDR bearings with thicker rubber layers were more effective in reducing the deflection in the lower slab layer. The deformed isolators of each building under compression are shown in Figure 40.

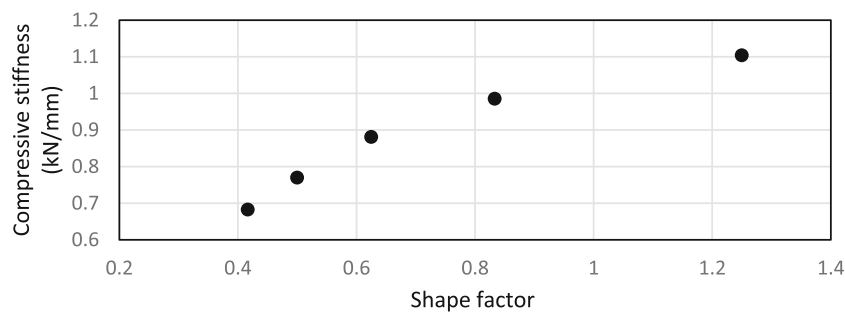


FIGURE 36 Effect of shape factor on compressive stiffness of Hybrid Rubber-Concrete Isolation Slab System (HRCISS) in multistory building under half-cyclic loading

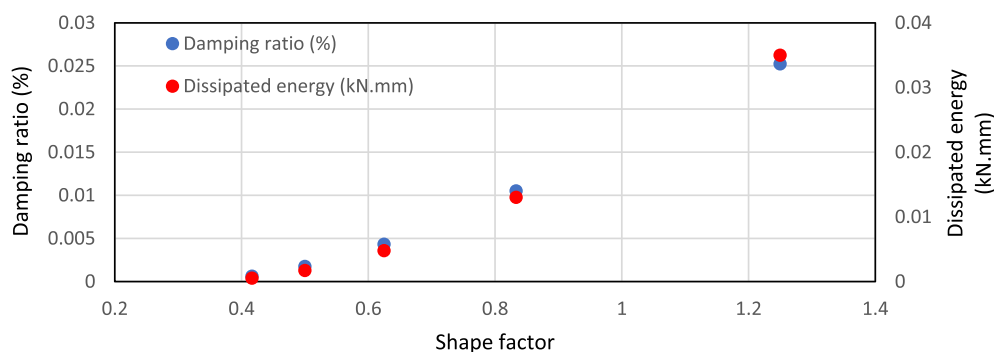


FIGURE 37 Effect of shape factor on dissipated energy and damping ratio of Hybrid Rubber-Concrete Isolation Slab System (HRCISS) in multistory building under vertical half-cyclic loading

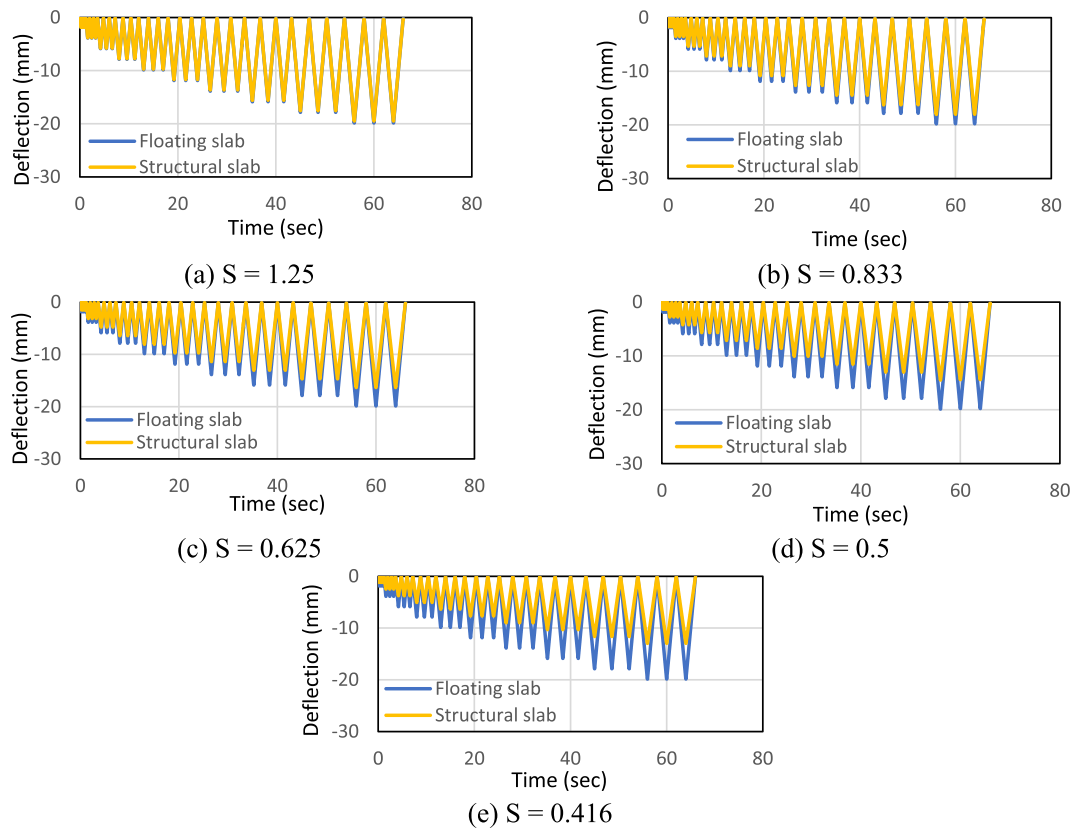


FIGURE 38 (a–e) Midpoint deflection of structural and floating slabs in buildings with HDRBs of different shape factor

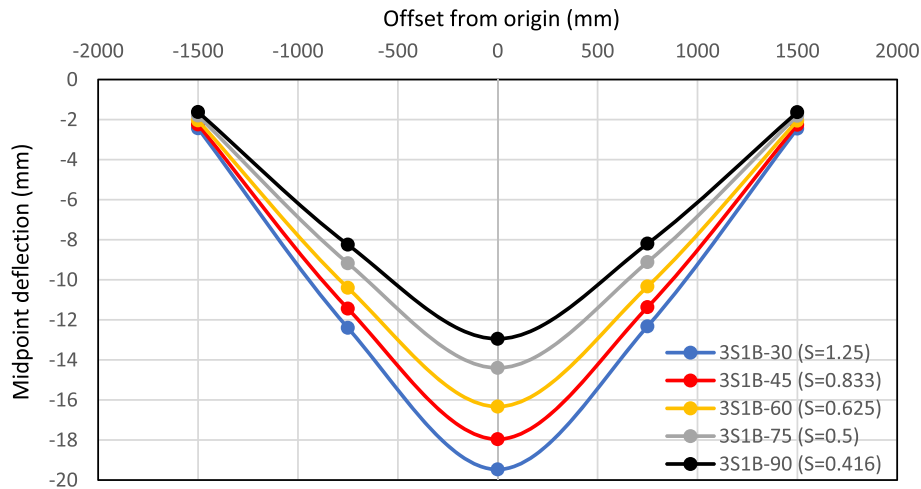


FIGURE 39 Deflection at mid, quarter and edge points of the structural slab in the multistory building with different rubber thickness (shape factors)

5.2 | Exterior vibrations testing

In this section, the influence of the shape factor on the HRCISS performance under exterior vibrations within a multistory building was investigated. The exterior vibrations were represented by 3D seismic components subjected at the building base.

Practically, the HDR bearings between the floating slab under the vibrating machine and the structural slab beneath have a dual function. The first function was to isolate the machinery from the induced vibrations at the building base and transmitted through the columns up to the

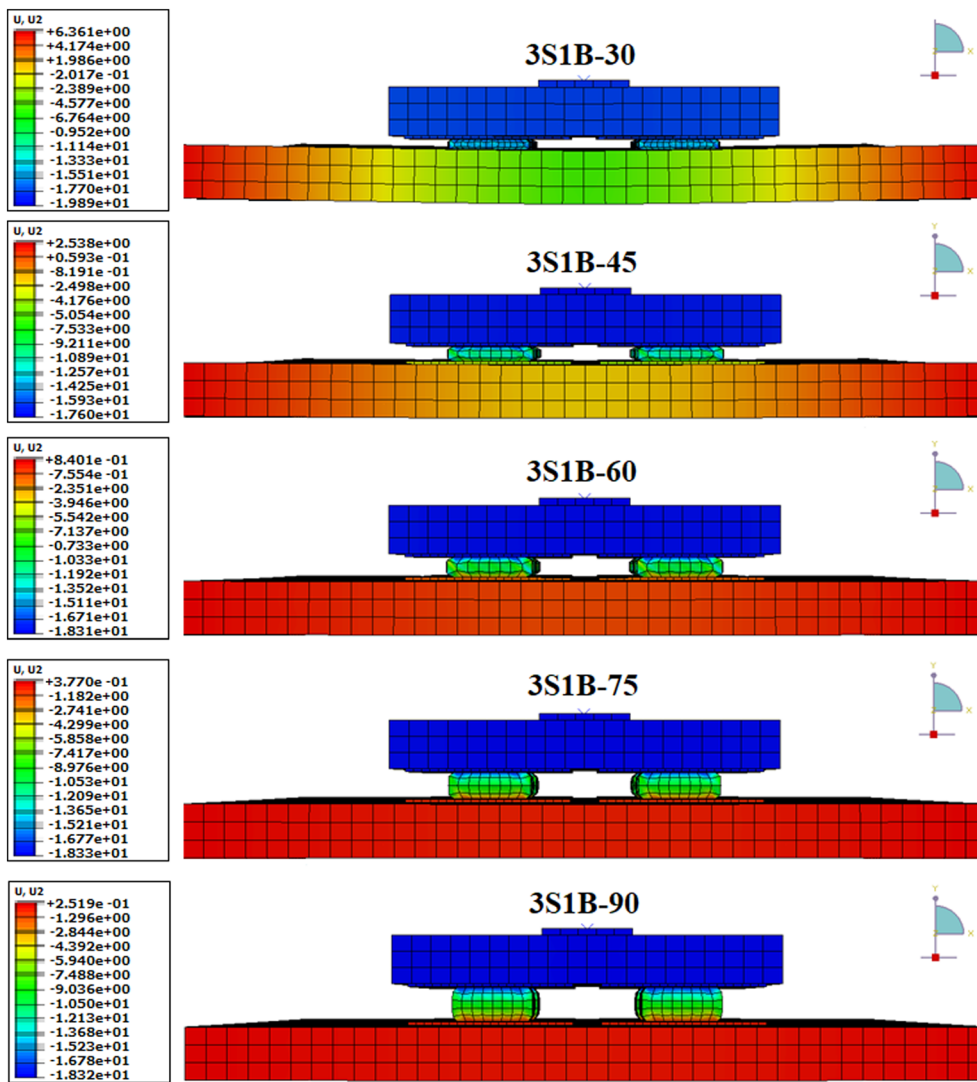


FIGURE 40 Close-up of High Damping Rubber (HDR) bearings deformation under cyclic compression in the multistory building with different rubber thicknesses (shape factors)

structural slab. Hence, the first task for the floating rubber-slab and the machine was to serve as a tuned mass damper (TMD) that mitigates the vibrations in the building stories and eventually minimizes the lateral and vertical deformations in the structural slabs. The second task was for the HRCISS to decouple vibrations on the floating slab, similar to a base-isolation (BI) system.

5.2.1 | HRCISS performance as tuned mass damper (TMD)

a. Effect of shape factor under El Centro North-South (N_S) horizontal seismic component

The lateral deformation of each story in the multistory building under the seismic loading in the north_south direction is shown in Figure 41. Comparisons between the different shape factors were based on the maximum lateral drift of the building's rooftop.

Additionally, Figure 41 a shows the horizontal drifts for the buildings with machine equipped in the 1st story in the direction of the North-South (N_S) component for the isolated and non-isolated buildings.

The vibration amplitude in some of the hybrid buildings exceeded that of the conventional building for a specific time period. This observation was also recorded in buildings with machines equipped in the second and third stories. Figure 42 illustrates the peak values of the rooftop lateral drift for the buildings with hybrid systems of different shape factors (bearing thickness) and different story level with respect to the conventional buildings.

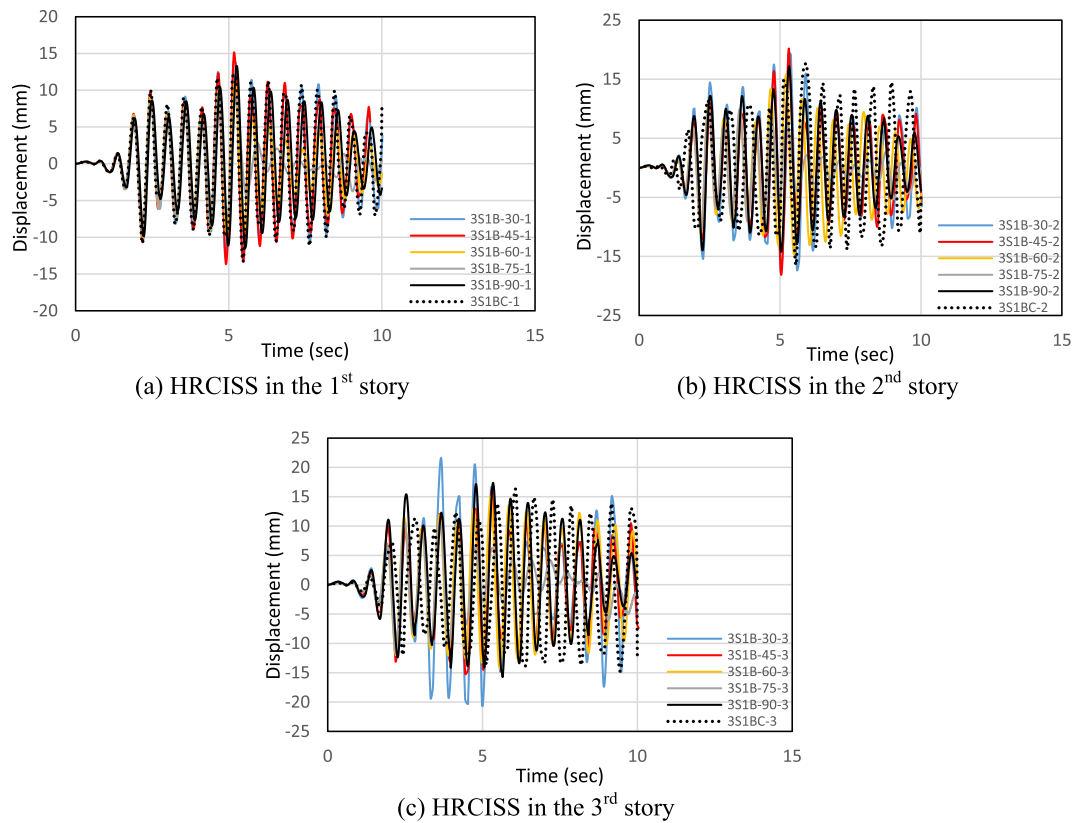


FIGURE 41 (a–c) Shape factor effect on the rooftop lateral displacement of the three-story one-bay building in the N_S direction

Figure 42 illustrates the effect of bearing thickness (shape factor) on the rooftop's maximum lateral drift in comparison with the buildings with non-isolated machines. Notably, the maximum lateral drift of hybrid buildings was reduced for buildings with bearings thicker than or equal to 60 mm ($S \geq 0.625$). This is the case in buildings with HRCISS mounted in first, second, and third story level. However, the maximum drift in the third story-equipped hybrid building was also reduced for bearings with 45-mm thickness ($S = 0.833$).

The peak drifts in 3S1B-60-1, 3S1B-75-1, and 3S1B-90-1 were reduced by 17.63%, 26.48%, and 0.45%, respectively, with respect to 3S1BC-1. While the maximum drift increased slightly in both 3S1B-30-1 and 3S1B-45-1 by 4% and 13.58%, respectively. In a similar scenario, the peak displacements in 3S1B-60-2, 3S1B-75-2, and 3S1B-90-2 dropped by 10.13%, 37.8%, and 2.22% to the lateral drift of 3S1BC-2 and increased by 10.53% and 14.4%, respectively, whereas in buildings with HRCISS mounted in the third story, the rooftop peak drift was reduced in 3S1B-45-3, 3S1B-60-3, 3S1B-75-3, and 3S1B-90-3 by 12.64%, 18.4%, 36.42%, and 5.86% and rose by 15.2% in 3S1B-30-3 with respect to 3S1BC-3.

The maximum amplitude of the rooftops was reduced in the hybrid buildings with bearings of lower shape factors but increased slightly above the conventional building's peak displacement for higher shape factors. This could be resulted from the varying mass, damping, and stiffness of the different rubber bearings, which can reduce the drift amplitudes for some thicknesses and increase it for the others under specific external stimulation (earthquake),^[28] such in case of 30- and 45-mm bearings, which resulted in higher maximum amplitudes than the conventional buildings. Additionally, the difference in reduction values of lateral drifts for hybrid systems mounted in different story levels may be a result to the distinct shear value in the structural slabs, of each story level, connected to the rubber bearings, and floating slab above.

b. Shape factor effect under El Centro East–West (E_W) horizontal seismic component

The East–West (E_W) acceleration-time history component of the 1940 El Centro earthquake strikes the building in the z-direction. As shown in Figure 43, the three-story one-bay building under such excitation deformed laterally. The story drift of the upper floor of the all five considered hybrid isolated buildings was compared with the conventional non-isolated building.

Although the E_W component is similar to the N_S component for hitting the building laterally, the HDR bearings in the z-direction decreased the maximum lateral displacement for all the hybrid buildings compared to the non-isolated. The decrement rate was different for the different shape factors and was the lowest for bearings with 60-mm thickness. The HRCISS was most effective in reducing lateral drifts when installed in the first story, especially for bearings thicker than or equal to 60 mm, while it had a slight influence for thinner bearings ($S \geq 0.833$).

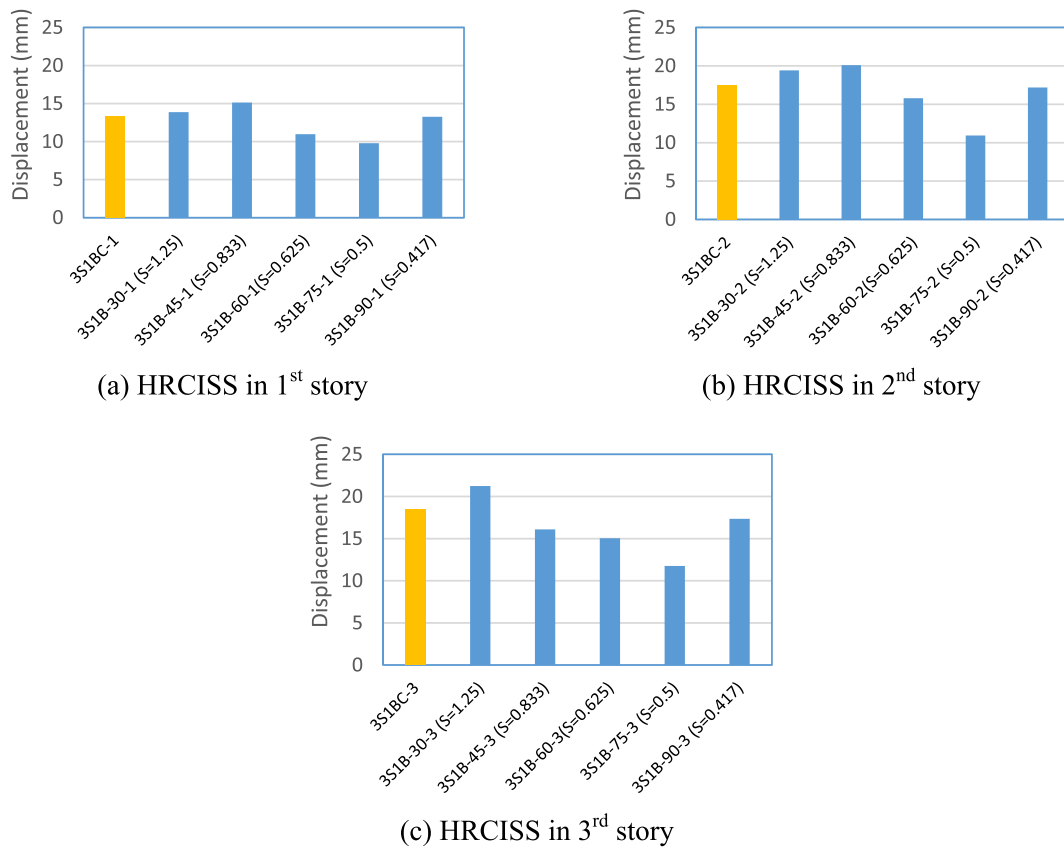


FIGURE 42 (a–c) Maximum rooftop lateral displacement in the N_S direction for buildings with isolated and non-isolated machines with bearings of different shape factors and mounted in different story levels

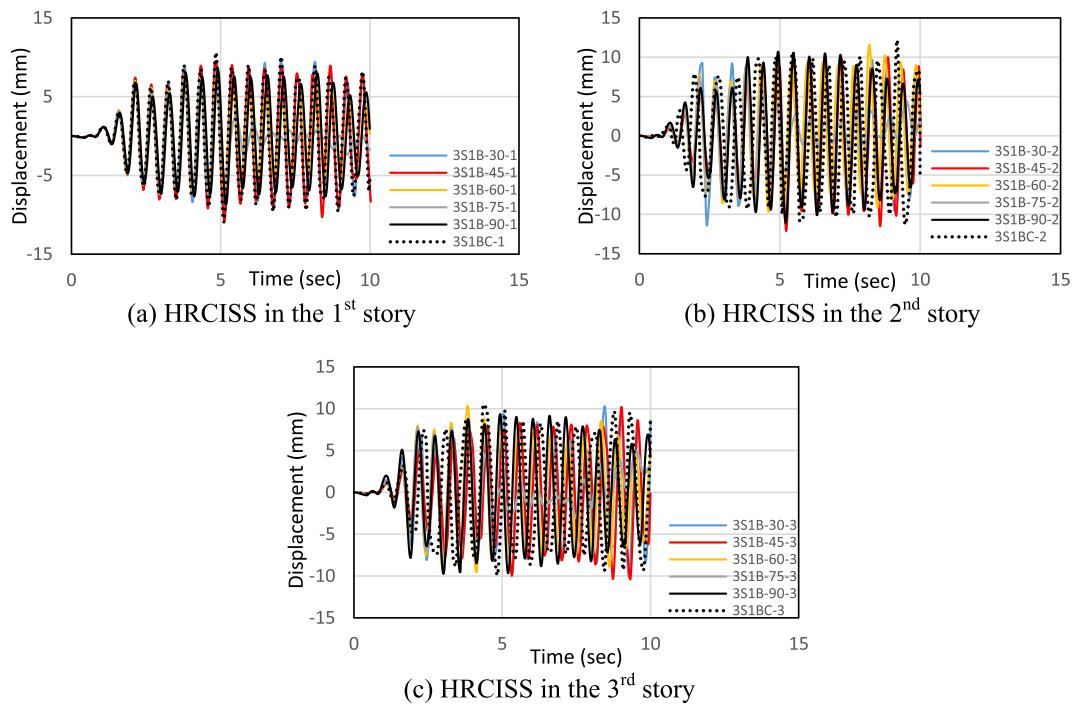


FIGURE 43 (a–c) Shape factor effect on the rooftop lateral displacement of the three-story one-bay building in the E_W direction

For the first story-installed rubber layer, the reduction of the story drifts for 3S1B-30-1 to 3S1B-90-1 were 8.27%, 5.32%, 44.46%, 41.15%, and 37.34%, respectively, compared to 3S1BC-1. Meanwhile, the reduction in drift with respect to 3S1BC-2 were 8.95%, 0.82%, 5.26%, 26.71%, and 9.12% for 3S1B-30-2 to 3S1B-90-2, in respective order. Likewise, for the hybrid system set in the upper story beneath the vibrating machine, the lateral drift values slightly dropped in comparison to 3S1BC-3 to 3.65%, 0.67%, 0.96%, 15.46%, and 6.53% for 3S1B-30-3, 3S1B-45-3, 3S1B-60-3, 3S1B-75-3, and 3S1B-90-3, respectively. Figure 44 demonstrates the reduced drift amplitudes with respect to the conventional.

In contrast to the lateral drifts under N_S component, the bearings installed in the first story under the E_W component had the highest drift reduction rate while the bearings set in the third story under the N_S component had the highest drift reduction rate. The contradicted behavior under the N_S and E_W components could be a result of the distinctive acceleration values for specific time periods of the two components that are striking the building simultaneously and leading to opposite outcomes.

c. Shape factor effect under El Centro up-down (U_D) vertical seismic component

According to the plotted pattern of the vertical midpoint displacement of the structural slab of each building shown in Figure 45, the structural slab of the conventional building recorded the least deflection. This may be due to the less mass carried by the slab compared to other hybrid buildings that contain HDR layers in addition to the floating slab and the vibrating machine mass. Although the extra mass of the bearings caused an apparent increment in the deflection, the difference between the displacement amplitudes during the vertical pushing and release decreased for hybrid buildings compared to the conventional building slab. The rate at which the difference in vibration dissipates depends on the shape factor of the HDR bearings. This was valid for all HRCISS levels, as the behavior of the structural slabs was not largely affected by the level of the story, where the machine and the hybrid system were installed. Buildings with the smallest bearing thicknesses, $H = 30$ mm and $H = 45$ mm (corresponding to the highest shape factors, $S = 1.25$ and $S = 0.833$) recorded less deflection but a higher difference between the vibration amplitudes. In contrast, buildings with higher bearing thickness (lower shape factors) resulted in more deflected structural slabs and smaller gradual differences in vibration over time.

Nevertheless, buildings 3S1B-90-1, 3S1B-90-2, and 3S1B-90-3 showed less deflection with respect to two other buildings of smaller bearing thickness. Notably, the structural slab of all hybrid buildings, except for buildings with 60- and 75-mm bearings thickness, displaced vertically to a certain value within the first second of the earthquake vertical component and afterward vibrate within the same displacement value range.

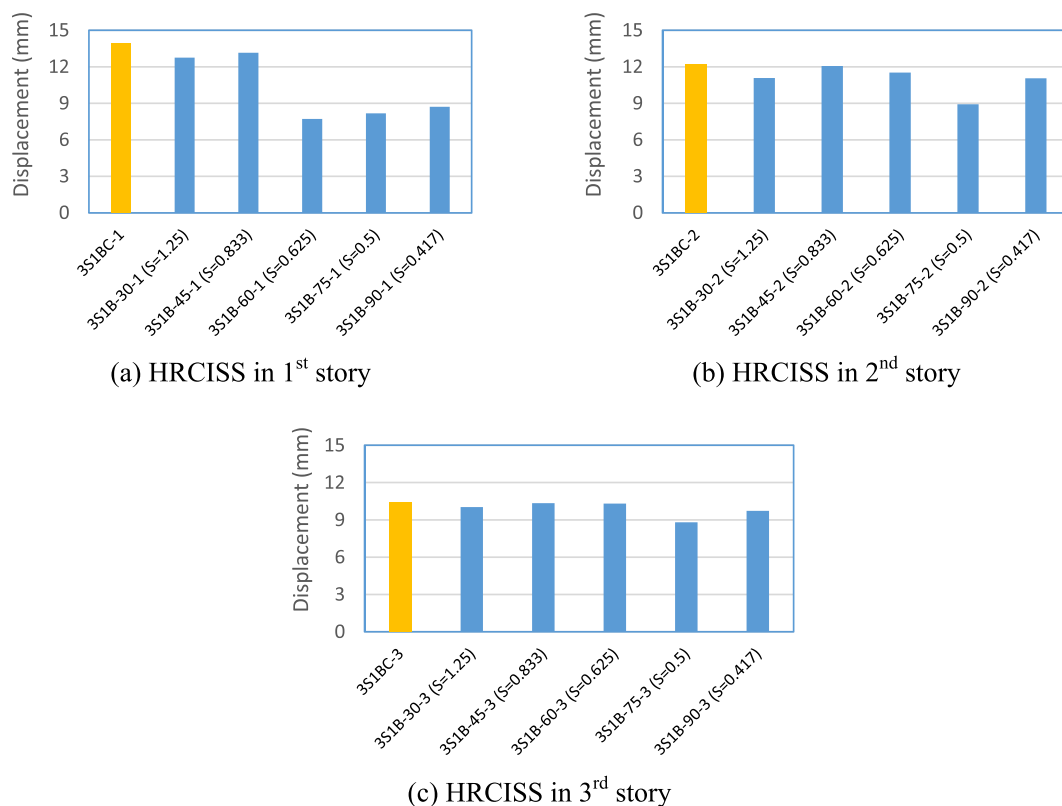


FIGURE 44 (a–c) Shape factor effect on the rooftop lateral displacement in the E_W direction for different Hybrid Rubber-Concrete Isolation Slab System (HRCISS) levels

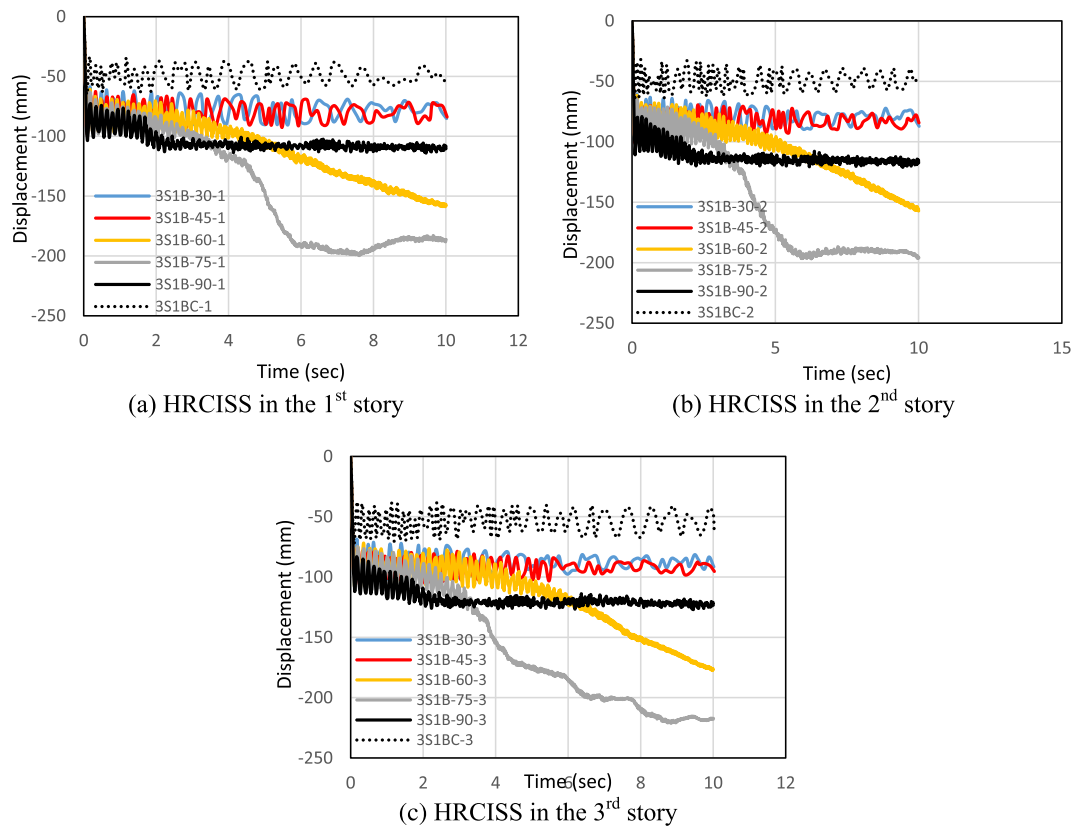


FIGURE 45 (a–c) Shape factor effect on the midpoint vertical displacement in the structural slab of the three-story one-bay building in the U_D direction

However, buildings 3S1B-60 and 3S1B-75 showed distinct behavior, where their structural slabs displaced downwards, which corresponded gradually with the seismic excitation but the range of their vibration amplitudes decreased with respect to time. The structural slab of the conventional buildings 3S1BC1, 3S1BC2, and 3S1BC3 was the least vertically displaced but measured the largest vibration amplitudes difference.

5.2.2 | HRCISS performance as a base-isolation (BI)

As an isolation layer, the HDR bearings under the floating slab and the generating machine separate the floating slab above and the structural slab beneath. The soft and damping characteristics of the rubber layers help to reduce the vibration amplitudes transmitting from the structural slab to the isolated slab, therefore protecting the vibrating machinery from seismic deformation. The shape factor has a marginal influence on the reduction in vibration amplitudes between the structural and floating slabs under the N_S, E_W, and U_D components of the 1940 El Centro earthquake. Table 6 shows the reduction of the 3D deformation of the floating slab with respect to the structural slab deformations. A specific pattern can be seen in all three directions. The lateral and vertical displacements values of the floating slab decreased in a building with the same shape factor value with the increment in the level of the machine-equipped story compared to the structural slab of that story. However, the reduction value for buildings with the same machine-equipped story level increased with the augmentation in the HDR bearing thickness (decrement in shape factor). The relationship between the different bearings' story levels and shape factors is portrayed in Figure 46.

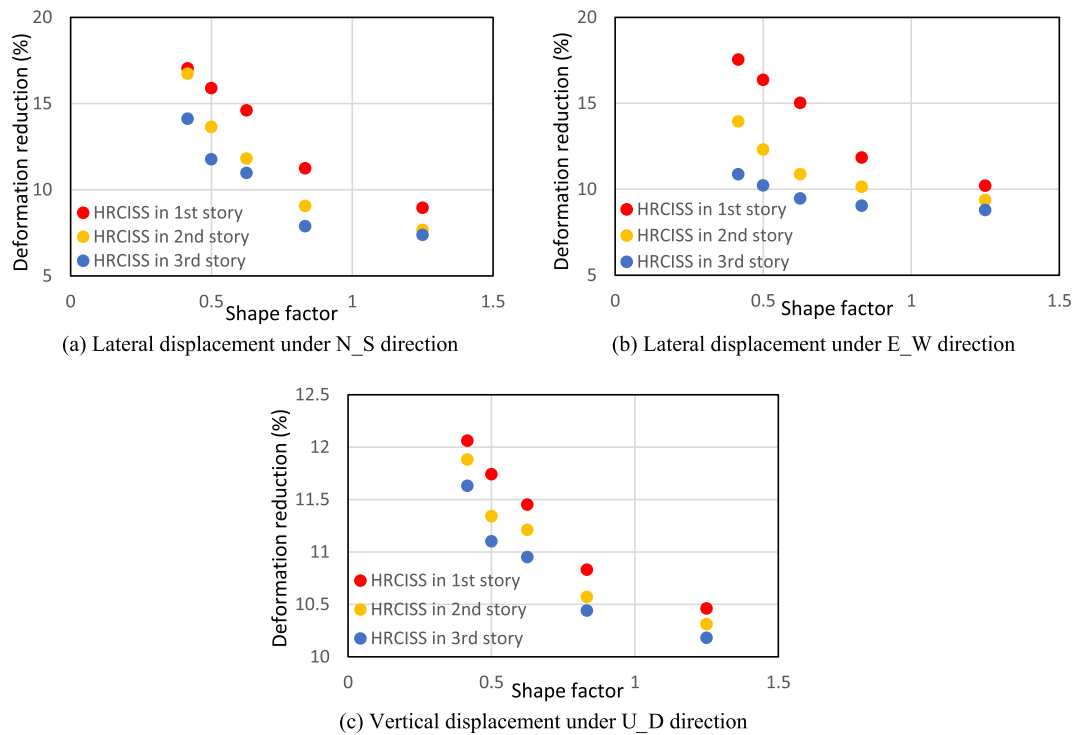
6 | APPLICATION OF HRCISS ON A TWO-STORY TWO-BAY BUILDING

For further validation of the current model, a real-life as-built RC frame with a shaker at top story, which was experimentally tested and studied by Shin et al.^[29] is selected for the FE modeling. The frame is a two-story two-bay building (Figure 47) with dimensions' details demonstrated at Figure 48. The frame was designed using the FE software and the dimensions and material properties were defined based on the real structure. Then the HRCISS (with rubber bearings with 60-mm thickness) (similar to the experimental specimens in current research) was installed in the

TABLE 6 Effect of shape factor on the 3D deformation value in floating slab with respect to the structural slab respective deformation

El Centro 1940 component	Machine-equipped story	Deformation reduction (%)				
		$H = 30 \text{ mm}^a$ $S = 1.25$	$H = 45 \text{ mm}$ $S = 0.833$	$H = 60 \text{ mm}$ $S = 0.625$	$H = 75 \text{ mm}$ $S = 0.5$	$H = 90 \text{ mm}$ $S = 0.416$
N_S	1st	8.95	11.24	14.6	15.89	17.03
	2nd	7.67	9.06	11.8	13.64	16.73
	3rd	7.38	7.88	10.97	11.76	14.11
E_W	1st	10.2	11.84	15.02	16.36	17.54
	2nd	9.73	10.14	10.88	12.31	13.94
	3rd	8.79	9.04	9.46	10.22	10.87
U_D	1st	10.46	10.83	11.45	11.74	12.06
	2nd	10.31	10.57	11.21	11.34	11.88
	3rd	10.18	10.44	10.95	11.1	11.63

^aH: HDR bearing thickness, S: Shape factor, N_S: North south, E_W: East west, and U_P: Up and down.

**FIGURE 46** (a–c) Effect of shape factor on deformation reduction in the floating slabs for the three-story one-bay buildings under El Centro 1940 3D components

middle of the top floor in the same location of the shaker in the real structure (Figure 49) and the sine pulse SP8 (of 203 mm amplitude) was applied on the HRCISS slab.

The analysis results in terms of lateral displacement of the 1st and 2nd stories for the structure with HRCISS are shown in Figure 50a. Accordingly, the peak inter-story drift ratio of frame utilized with HRCISS slab were calculated and compared with results of the retrofitted structure by Shin et al.^[29] as shown in Figure 50b. These results illustrate the peak inter-story drifts of both frames and indicates that the reduction in drift in both story levels of the structure occurred where the developed rubber bearings were used. This demonstrates that dissipating effect of the sine pulse on the structure by rubber bearings outperforms in comparison to the retrofitting of the structure's columns, which is very costly. The reduction in the peak inter-story drifts for the first and second stories were about 12.15% and 6.22%, respectively compared to the retrofitted building.



FIGURE 47 Four identical two-story, two-bay frames^[29]

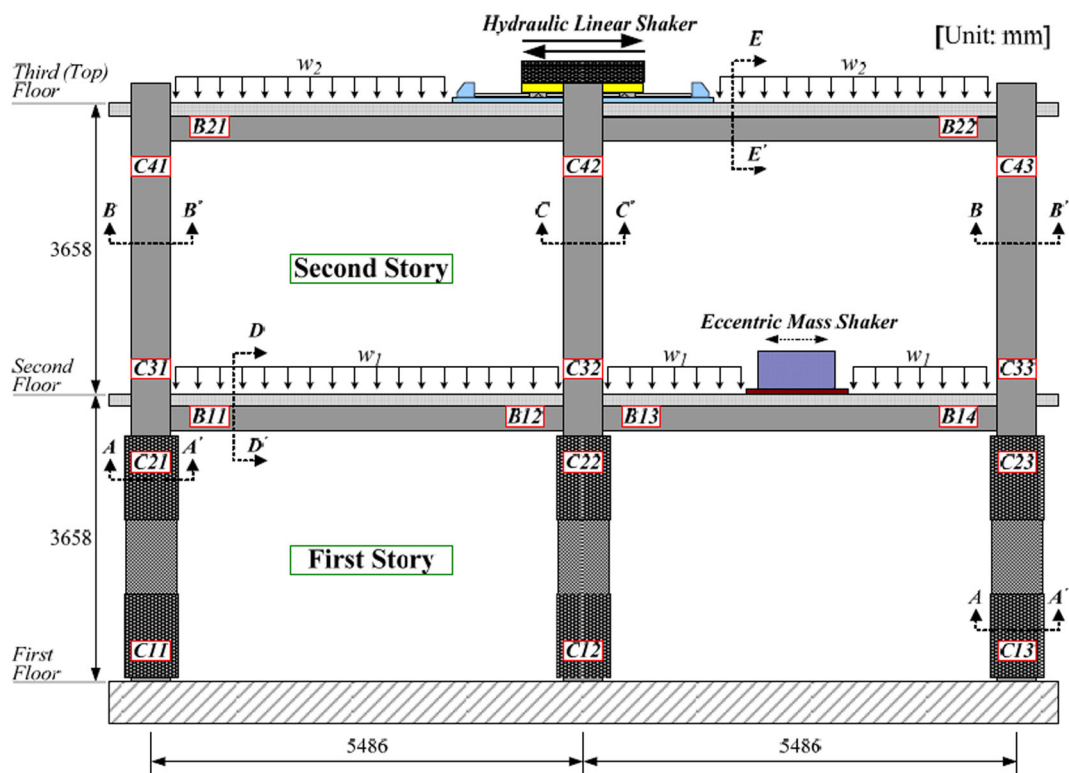


FIGURE 48 Test frame details^[29]

7 | LIMITATIONS AND ADVANTAGES OF THE PROPOSED HRCISS SLAB

The limitations of the proposed system can be summarized as follows:

- i. This system is applicable to vibrations with low to moderate frequency since there is no action by rubber component in applied high frequency vibrations with negligible movement.

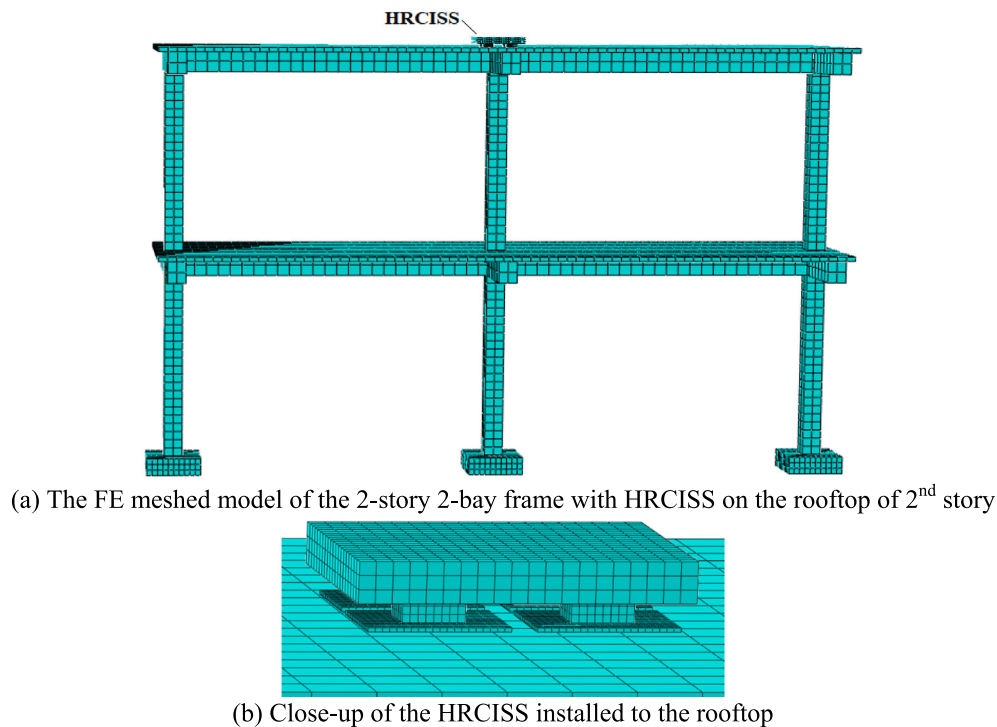


FIGURE 49 (a and b) The two-story two-bay as-built frame modeled and meshed via finite element (FE)

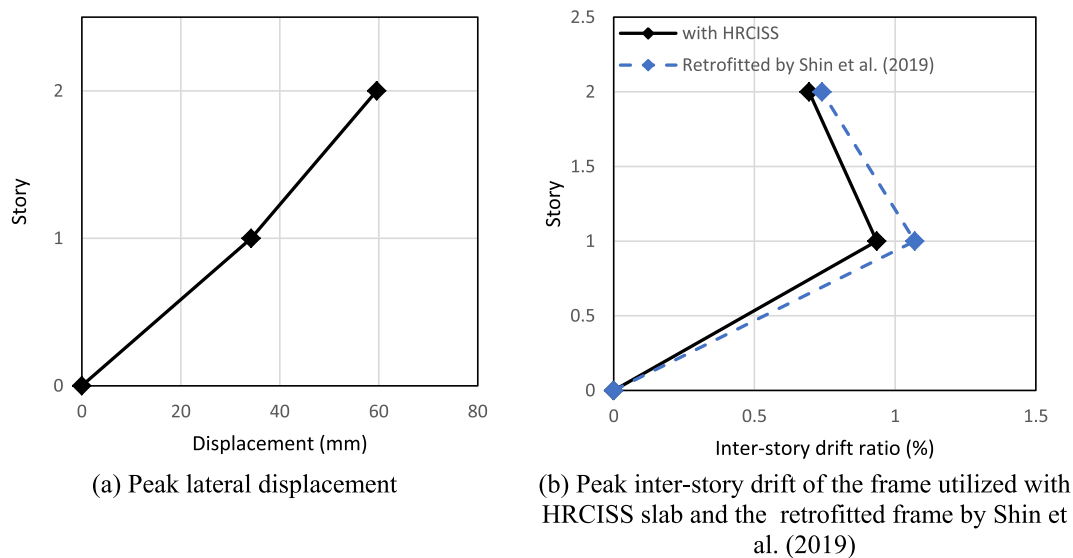


FIGURE 50 (a and b) Peak displacement and inter-story drift ratios of the Hybrid Rubber-Concrete Isolation Slab System (HRCISS)-mounted frame and the column-retrofitted frame by Shin et al.^[29]

- ii. The proposed system functions for vibrations with amplitude range between 50% and 200% shear strain of rubber thickness due to rubber properties.
- iii. The proposed system is applicable for flat slabs only and for inclined slabs the rubber performance may be affected by the overturning moments.
- iv. The system composes four rubber bearings only due to the nodal points determined by the natural frequency test on square plates.
- v. The proposed system is designed to carry low to moderate masses since the rubber material has been used only. Hence, to accommodate heavy payloads, the vertical stiffness of the HDR bearings can be increased by implementing the steel shims.

Whereas the limitations of this research work are summarized as follows:

- i. In the experimental testing, applied vibration amplitude to the specimens is limited due to restriction of stroke for the horizontal and vertical actuators. However, the slabs are cracked before experience of maximum stroke of actuator.
- ii. Dimension of the lower slab in experimental test was dependent on the arrangement of bolts in the strong floor, whereas the upper slab's size is minimized (in comparison to the lower slab) in order to avoid of any contact with the strong floor bolts during pushing and pulling operation.
- iii. Conducting experimental test simultaneously for both horizontal and vertical movement for the slab was not done due to limitation of facilities for connecting the two actuators to the slab at the same time. Therefore, experimental tests have been done individually for horizontal and vertical movement using two identical slabs.
- iv. This study focused on implementing square rubber bearings, however circular rubber bearings may exhibit different response. Also, dimension of rubber bearing (rubber section area) may lead to different responses.
- v. Since conducting full scale experimental testing for the frame with proposed slab with rubber bearing is required special equipment, therefore only FE method was used for simulation of three-story one-bay building and investigate its response under applied loads.
- vi. In this study only three-story frame equipped with proposed slab system has been considered to study due to limited computational facilities; however, application of the slab with rubber bearing in high rise buildings may lead to the more interesting results.

The advantages of the proposed HRCISS slab system can be summarized as follows:

- i. Simple design and low cost for manufacturing of the square-section rubber bearings (without of the steel shims).
- ii. The capability of installing the proposed isolation slab system in existing buildings without the need of reconstruction.
- iii. The system can carry low to medium weight machines and extendable to accommodate heavy machines by adding steel shim plates to the rubber bearing.
- iv. The proposed HRCISS slab able to exhibit dual performance to dissipate vibrations of the generating machines as isolator system and also diminish effect of ground motion and structural excitation as TMD.
- v. The proposed system is acting against applied bi-axial excitation (both horizontal and vertical movement) to protect the structure under applied realistic loads.

8 | CONCLUSION

This study has successfully investigated the development of the HRCISS for building structures subjected to multidirectional vibrations on various story levels and determined the effect of shape factors in the proposed system under horizontal and vertical vibrations. Several significant findings that can be highlighted are as follows:

1. The shape factor of the HDR bearings demonstrated a huge effect on the dynamic response of the HRCISS under both interior and exterior vibrations when applied in a multistory building.
2. Under interior vibrations (machine-induced 3D vibrations), the lateral drift of the three-story one-bay building decreased with the decrement of shape factor with as buildings with machines and HRCISS installed in the 1st story recorded more reduction.
3. Likewise, the deflection in the structural slab under the HRCISS decreased for lower shape factor bearings. However, the reduced deflection was not largely influenced by the level of the machine-equipped story. Additionally, the rubber layer became stiffer in shear and compression directions with a higher shape factor.
4. HDR bearings with higher shape factors showed a tendency to dissipate more energy in the shear and compression for lower machine-equipped story levels.
5. The damping ratio also increased for higher shape factors in all directions. A lower leveled machine-equipped story becomes more damped in compression. However, the damping ratio was the highest for HRCISS installed in the second story.
6. The shape factor was notably influential on the 3D deformation under exterior vibrations (seismic induced vibrations), where the HRCISS functioned as a TMD.
7. Lateral drift in the N_S and the E_W directions were slightly reduced with the reduction in the shape factor and rose again for the 90 mm HDR bearings (corresponding to the lowest shape factor, $S = 0.416$) and the largest decrement for the 75-mm HDR bearings ($S = 0.5$). The HRCISS equipped in the first story achieved the optimal reduction for both lateral directions, while the decreasing shape factor led to a more deflected structural slab under the vertical seismic component up to the maximum deflection for the 75-mm HDR bearings. However, the difference between the maximum and minimum displacement amplitudes decreased with the decreasing shape factors.

8. In the case of HDR bearings functioning as a BI, the shape factor decrement increased the deformation reduction in the structural slabs of the machine-equipped stories with respect to the floating slab deformation in all three dimensions.
9. The HRD bearings reduced the peak inter-story drift when applied numerically on an as-built two-story two-bay frame compared to an actual retrofitted identical frame.

DATA AVAILABILITY STATEMENT

Data sharing is not applicable to this article as no datasets were generated or analyzed during the current study.

ORCID

Farzad Hejazi  <https://orcid.org/0000-0002-7725-5568>

REFERENCES

- [1] F. Naeim, J. M. Kelly, *Design of Seismic Isolated Structures: From Theory to Practice*, John Wiley & Sons, New York 1999.
- [2] F. Khoshnudian, D. Motamedi, *KSCE J. Civ. Eng.* **2013**, 17(6), 1333. <https://doi.org/10.1007/s12205-013-0115-5>
- [3] M. S. Chalhoub, J. M. Kelly, *Int. J. Solids Struct.* **1990**, 26(7), 743.
- [4] H. S. Soleimanloo, M. A. Barkhordari, *Trends Appl. Sci. Res.* **2013**, 8(1), 14. ISSN 1819-3579/DOI: 103923/tasr.2013.14.25.
- [5] G. P. Warn, B. Vu, "Exploring the low shape factor concept to achieve three-dimensional seismic isolation", *20th Analysis & Computation Specialty Conference*, ASCE, 1–11, **2012**.
- [6] E. Sato, K. Kajiwara, S. Furukawa, X. Ji, M. Nakashima, "Full-scaled shaking table test of a hospital made of base-isolated four-story concrete structure" Proceedings from the 9th US National and 10th Canadian Conference on Earthquake Engineering, Toronto CA, **2010**.
- [7] X. Ren, W. Lu, Y. Zhu, S. Günay, *Struct. Design Tall Spec. Build.* **2020**, 29(13), e1773.
- [8] A. Khaloo, A. Maghsoudi-Barmi, M. E. Moeini, *Structures* **2020**, 26, 456. Elsevier.
- [9] F. Cilento, R. Vitale, M. Spizzuoco, G. Serino, A. Muhr, *Ing. Sismica* **2017**, 36(2), 86–1022019.
- [10] D. Losanno, I. E. Madera Sierra, M. Spizzuoco, J. Marulanda, P. Thomson, *Eng. Struct.* **2019**, 209, 110003.
- [11] D. Losanno, A. Calabrese, I. E. Madera Sierra, M. Spizzuoco, J. Marulanda, P. Thomson, G. Serino, *J. Earthq. Eng.* **2020**, 26, 1921. <https://doi.org/10.1080/13632469.2020.1748764>
- [12] K. N. Klafas, S. A. Mitoulis, *Procedia Eng.* **2017**, 199, 2979.
- [13] E. Tubaldi, S. A. Mitoulis, H. Ahmadi, *Soil Dyn. Earthq. Eng.* **2018**, 104, 329.
- [14] J. Oh, J. H. Kim, *J. Vibroengineering* **2017**, 19(1), 355.
- [15] K. Morita, M. Takayama, *12th World Conf. Earthq. Eng.* **2000**, 6, 1838.
- [16] S. R. Moghadam, D. Konstantinidis, *Compos. Struct.* **2017**, 163, 474.
- [17] J. Sunaryati, A. Adnan, M. Z. Ramli, "Evaluation of the laminated hollow circular elastomeric rubber bearing", *The 14th World Conference on Earthquake Engineering*, Beijing, China, **2008**.
- [18] J. Lee, T. Shin, G. Koo, "Design approach of laminated rubber bearings for seismic isolation of plant equipment", Easy Chair, No. 2447, **2020**.
- [19] O. Gauron, A. Saidou, A. Busson, G. H. Siqueira, P. Paultre, *Eng. Struct.* **2018**, 174, 39.
- [20] ACI 318, *Building Code Requirements for Structural Concrete and Commentary*, American Concrete Institute; Farmington Hills, MI, USA **2014**.
- [21] International Organization of Standardization (ISO), (2005), "Elastomeric seismicprotection isolators. Part 1: test methods".
- [22] H. Jin, S. Zhou, W. Liu, *J. Vibroengineering* **2015**, 17(6), 3237.
- [23] C. K. Hui, C. F. Ng, *J. Sound Vib.* **2007**, 193(1), 175.
- [24] F. Hejazi, K. C. Tan, *Conceptual Theories in Structural Dynamics*, Springer, Singapore **2020**.
- [25] ACI T1.1-01, *Acceptance Criteria for Moment Frames Based on Structural Testing*, American Concrete Institute, Farmington Hills **2001**.
- [26] BS EN-1992-1-1, (2004), Eurocode 2: Design of Concrete Structures – Part 1–1, 186–187.
- [27] B. Yoo, J. H. Lee, G. H. Koo, *Comparison of Analysis Results With Experimental Results for ENEA and CRIEPI Rubber Bearings*, KAERI, Republic of Korea **1996**.
- [28] M. Khazaei, R. Vahdani, A. Kheyroddin, *Shock. Vib.* **2020**, 2020, 1.
- [29] J. Shin, J. S. Jeon, T. R. Wright, *Compos. Struct.* **2019**, 226, 111207.

How to cite this article: N. K. Fayyadh, F. Hejazi, *Struct Design Tall Spec Build* **2023**, 32(4), e1995. <https://doi.org/10.1002/tal.1995>